

N81-27948

(NASA-CR-160548) SOLID STATE CRYSTAL  
PHYSICS AT VERY LOW TEMPERATURES Final  
Report, 1 Jul. 1979 - 30 Jun. 1980 (Maryland  
Univ.) 64 p HC A04/MF A01 CSCL 20L

N81-27948

Unclas  
G3/76 26778

FINAL REPORT

To

NATIONAL AERONAUTICS AND SPACE ADMINISTRATION

On

SOLID STATE CRYSTAL PHYSICS AT VERY LOW TEMPERATURES

NSG 7196

W. Davis, K. Krack, J.-P. Richard and J. Weber

July 1, 1979 to June 30, 1980



UNIVERSITY OF MARYLAND  
DEPARTMENT OF PHYSICS AND ASTRONOMY  
COLLEGE PARK, MARYLAND

FINAL REPORT

To

NATIONAL AERONAUTICS AND SPACE ADMINISTRATION

On

SOLID STATE CRYSTAL PHYSICS AT VERY LOW TEMPERATURES

NSG 7196

W. Davis, K. Krack, J.-P. Richard and J. Weber

July 1, 1979 to June 30, 1980

## TABLE OF CONTENTS

	Introduction . . . . .	1
I	Crystal Experiments at T~4K.	
	Introduction . . . . .	2
	Description of Experiment . . . . .	4
	A. Crystal, Suspension, and Transducer	
	B. Q Measurements	
	C. Frequency Measurements	
	D. Cryogenics	
	E. Temperature Measurement and Control	
	Results of Q Measurements . . . . .	18
	Results of Frequency Measurements . . . . .	23
II	Crystal Experiments at T < 4K.	
	Introduction . . . . .	25
	Proposed Experiments . . . . .	26
	Outline of Proposed Experiments . . . . .	28
	Magnetic Levitation . . . . .	29
	Appendix I    Description of The S.H.E. Corporation Dilution Refrigerator. . . . .	36
	Appendix II    Design of The milli-Kelvin cryostat and completion of The S.H.E. gas handling system. . .	51

## INTRODUCTION

In recent years, techniques have been developed for growing large very nearly perfect crystals. The properties of these crystals are of great interest in learning more about the structure of matter, and that is the immediate objective of the low temperature physics research described here.

These crystals, together with the environment of a spacecraft, offer some exciting possibilities. Extension of the crystal growing technology to the zero g region is likely to result in even more perfect crystals. Instruments based in the properties of these crystals offer possibilities of doing new physics, in a spacecraft.

These crystals also offer the possibility of serving as references for an entirely new class of clock, orders more precise than an atomic hydrogen maser.

This report describes the ongoing crystal experiments at the University of Maryland. The first part describes the measurements of Q and frequency of a silicon crystal at temperatures of around 4K. The second part of this report describes work done for the continuation of these experiments to temperatures around 20 mK.

## PART I: CRYSTAL EXPERIMENTS AT T-4K.

### INTRODUCTION

The experiment described in this part is a continuation of the cryogenic measurements of the properties of monocrystals. Specifically, further measurements of the mechanical dissipation and resonant frequency of a 15 kg silicon crystal from 5 to 18 Kelvin are presented and discussed. There are three other papers which describe previous results in this series of ongoing experiments. They are entitled:

- 1) "Measurements of Dielectric Monocrystals at Cryogenic Temperatures"
- 2) "The Measurement of Noise in Monocrystals at Cryogenic Temperatures: Expected Problems and Proposed Solutions"
- 3) "Progress in the Measurement of Crystal Properties at Cryogenic Temperatures"

Paper (1) is the University of Maryland Physics Technical Report 79-069, PP 79-149. Papers (2) and (3) may be found in the University of Maryland Physics Preprint PP #81-016, entitled "Further Measurements of Dielectric Monocrystals at Cryogenic Temperatures."

Results presented in the previous papers suggest that the mechanical  $Q$  of the silicon crystal might not only depend on the temperature, but on the derivative of the temperature with respect to time. All previous  $Q$  measurements were made while the temperature was changing. In the experiment described in this paper, temperature control was incorporated to reduce the time derivative of the temperature. This reduced  $dT/dt$  by a factor of about ten. The results of the  $Q$  measurements with and without this temperature control are quite different. Because this difference is greater than

expected, other mechanisms for a change in  $Q$  are suggested. This needs further investigation.

In the previous report, measurements of the resonant frequency of the fundamental longitudinal mode of the silicon crystal from 6 to 300 Kelvin are presented and discussed. It was expected that the derivative of this frequency with respect to temperature,  $df/dT$ , be everywhere negative, i.e. frequency increasing as temperature decreases. This was observed down to about 16 Kelvin. However below this temperature the frequency decreased as temperature decreased, i.e.  $df/dT$  was positive. These measurements were repeated in the experiment described in this report, and the results were the same. It is suggested that this behavior is related to the coefficient of thermal contraction of silicon, which changes sign at 18 Kelvin.

## DESCRIPTION OF EXPERIMENT

The description of the experiment is divided into five parts:

- A. Crystal, Suspension, and Transducer
- B. Q Measurements
- C. Frequency Measurements
- D. Cryogenics
- E. Temperature Measurement and Control

### A. Crystal, Suspension, and Transducer

The silicon crystal which was used in this experiment was manufactured by Monsanto Corporation by the Czochralski process. It was p-type doped with boron,  $8 \times 10^{14}$  atoms/cm<sup>3</sup>. The length was 135 cm, diameter was 7.8 cm, and mass was 15.5 kg. The resonant frequency at room temperature was 3450.8 hz and at liquid helium temperatures was 3467.8 hz.

For the cryogenic experiments in this and the previous experiments, the crystal was supported as shown in figure 1. The four point suspension was machined from 6061 aluminum. It was 3.2 cm in diameter and length. Two pzt-4 piezoelectric ceramic transducers were epoxied onto the suspension with Stycast 2850 FT as shown in this figure. They were connected in series. Underneath the suspension were aluminum spacers and a base. A bolt went through the base, spacers, and suspension, where a nut was attached to hold the entire assembly tightly together. Mounted on the base were resistance thermometers and heater resistors for temperature measurement and control. Also mounted on the base was a thermal radiation shield used for temperature control. See figure 2. The base rested on a system of acoustic isolation shown in figures 2 and 3.

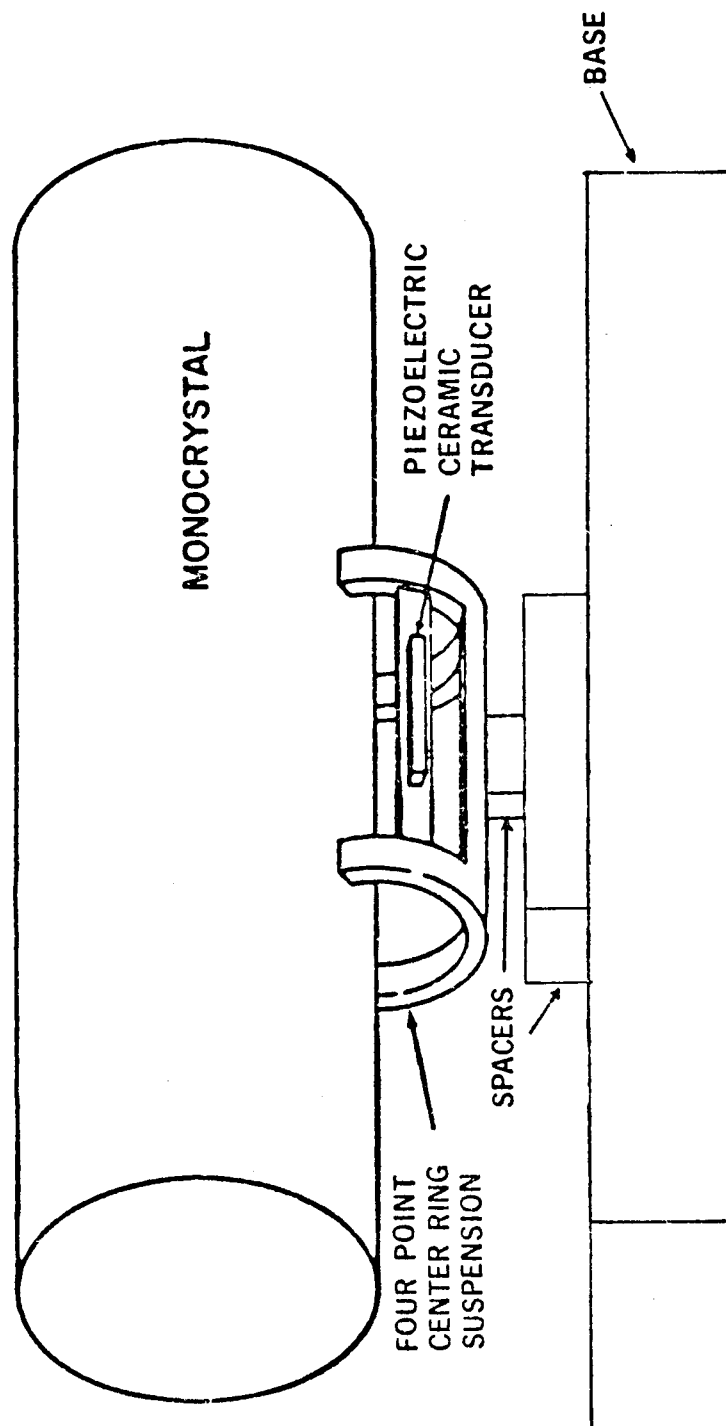


Figure 1. Four Point "Center Ring" Suspension



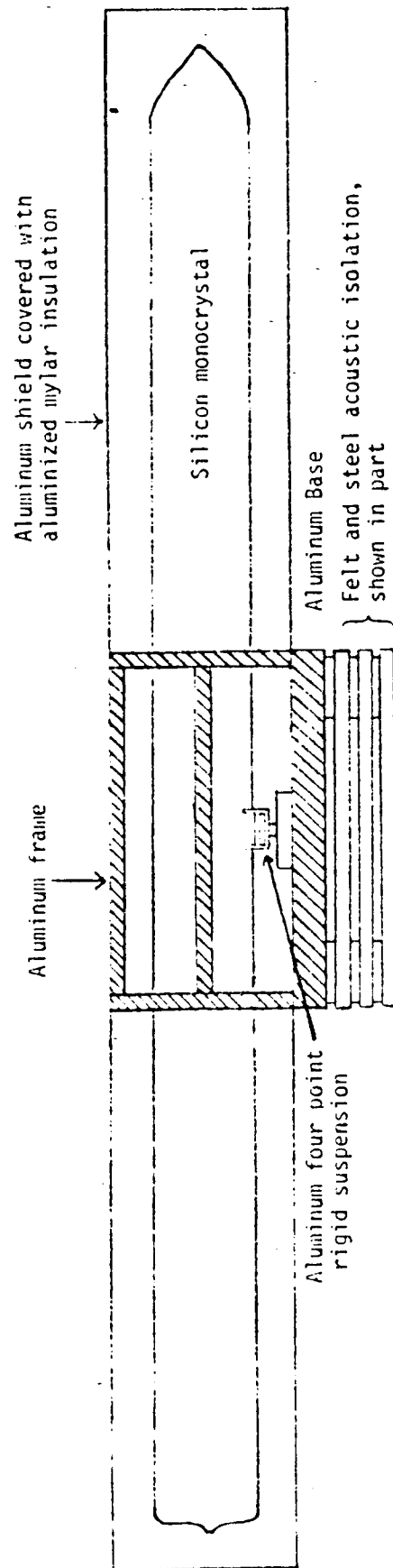


Figure 2. Thermal shield for temperature control of silicon.

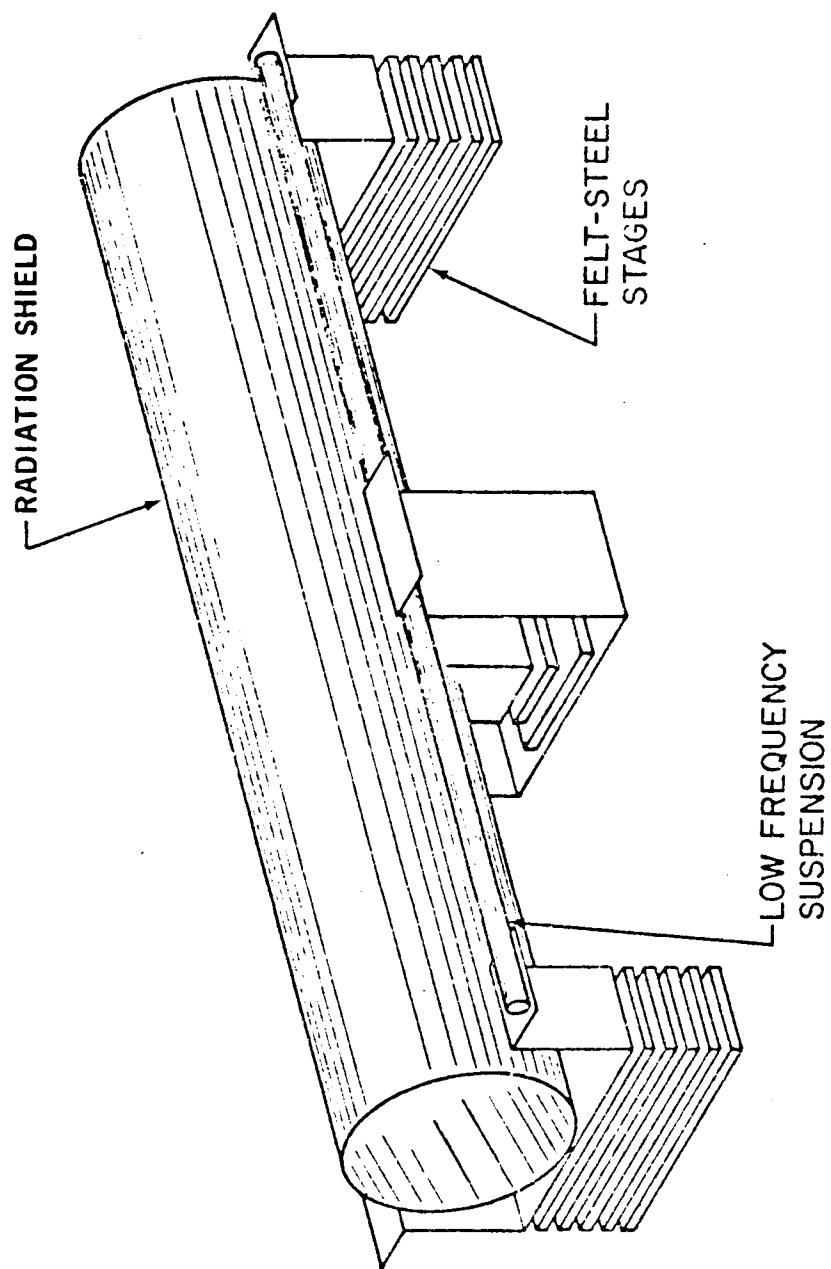


Figure 3. Crystal Isolation

## B. Q Measurements

Figure 4 shows a diagram of the electronics which were used for the Q measurements. The silicon crystal was excited by driving it at the resonant frequency with the transducer. Once excited, the crystal "rang" for hours. During this decay the transducer output was connected to a preamplifier shown in figure 5. The lock-in amplifier was set in the vector mode, which produced the magnitude of the input signal and the phase of the input signal with respect to the reference. A phase lock loop feedback circuit continuously adjusted the reference frequency generator to maintain this phase difference at zero. The phase lock loop had a damped second order response with respect to variations in phase difference. Thus the electronics could track the frequency and phase of the silicon crystal. The magnitude of the silicon oscillation was recorded on a chart recorder. Decay times ( $\tau$ ) and Q were computed from these recordings. The amplitude decays exponentially,

$$e^{-\frac{t}{\tau}}$$

If  $f$  is the frequency of the oscillation then the Q is given by,

$$Q = \pi \tau f$$

## C. Frequency Measurements

An electronic counter was used to measure the period of the reference generator which was tracking the period of the silicon oscillation. A 10 Mhz rubidium clock provided the external time base for the counter. A typical measurement was  $288,363,785 \pm 5$ . This was the number of 10 Mhz oscillations which were counted during a time interval of 100,000 oscillations of the silicon crystal, i.e. 28.8 seconds. The units of the measurement were picoseconds ( $10^{-12}$  sec).

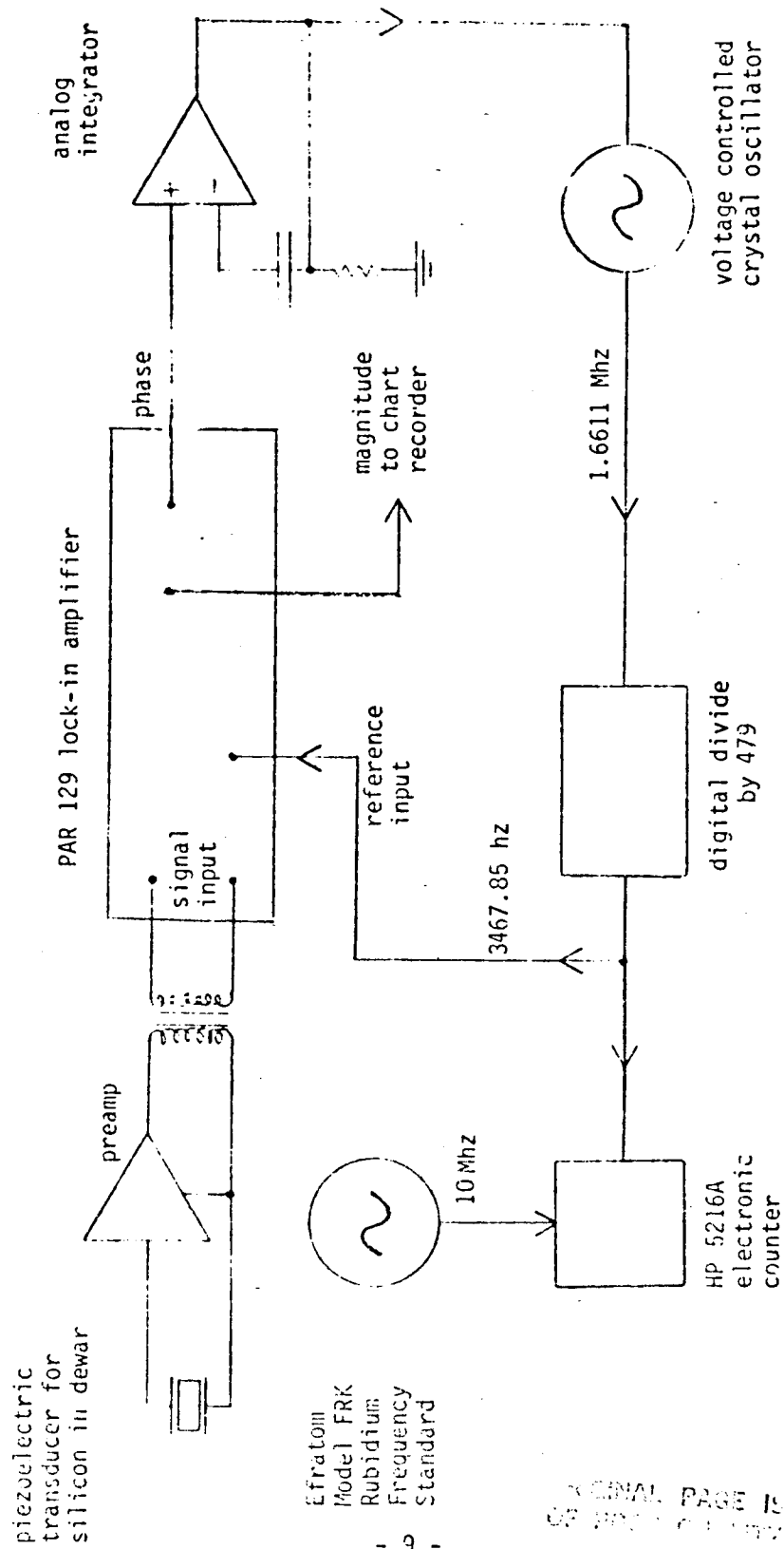


Figure 4. Electronics for silicon frequency and Q measurements.

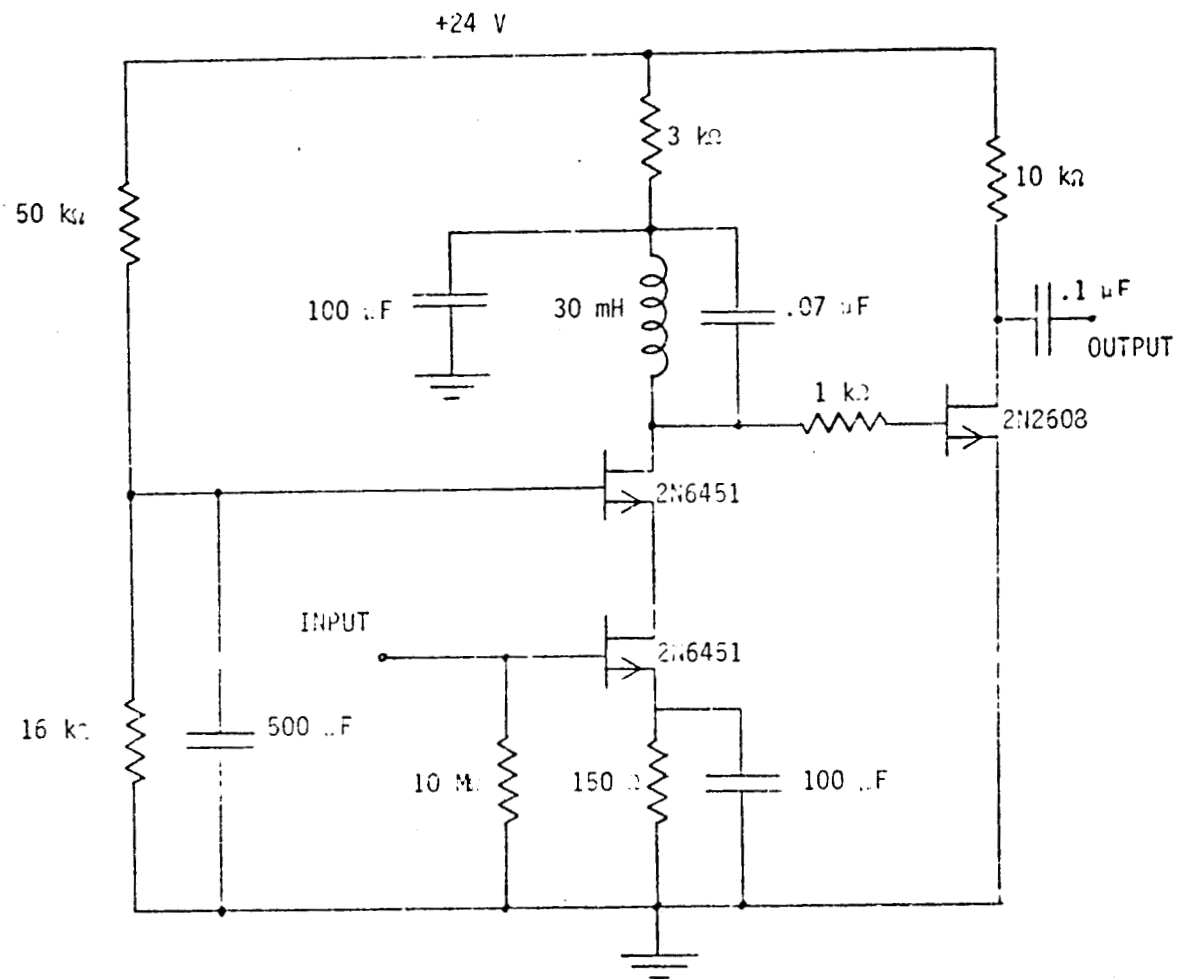


Figure 5. Preamplifier, Tuned Cascode, Typical Configuration

This example (at 5.12 Kelvin) corresponds to a frequency of  $3467.84186 \pm .00006$  hz. The error of a single measurement, one part in  $6 \times 10^7$ , was random and due to noise in the electronics during the counting interval. This error is almost four orders of magnitude larger than that expected for the rubidium time base over the same time interval. Furthermore the systematic error due to drift in frequency from change in temperature was also much less than the quoted random error. This random error,  $\pm 60$  phz, applies to all the frequency (period) measurements.

#### D. Cryogenics

A cross section of the cryostat is shown in figure 6. The dimensions of the experiment chamber were 48 cm in diameter and 163 cm in length. The experiment assembly shown in figure 3 fitted into this chamber. Here the experiment was cooled by cold helium gas and liquid in the dewar surrounding the chamber. Thermal conduction between the dewar and the experiment was accomplished by maintaining a pressure of a few microns of helium gas in the chamber. This gas was pumped out with a four inch diffusion pump, after the lowest temperature was reached. During the crystal measurements the pressure near the input of the pump was typically  $5 \times 10^{-6}$  torr as measured with a cold cathode gauge.

A Cryogenics Technology Model 1400 helium liquefier/refrigerator was used to cool the experiment and cryostat from room temperature to liquid helium temperatures and also to make liquid helium to fill the dewar. The helium vapor from the boiling liquid passed through and cooled the vapor shield, which provided an intermediate stage of shielding between the dewar and room temperature. This gas was then recovered and stored, so that the system could operate in a closed cycle.

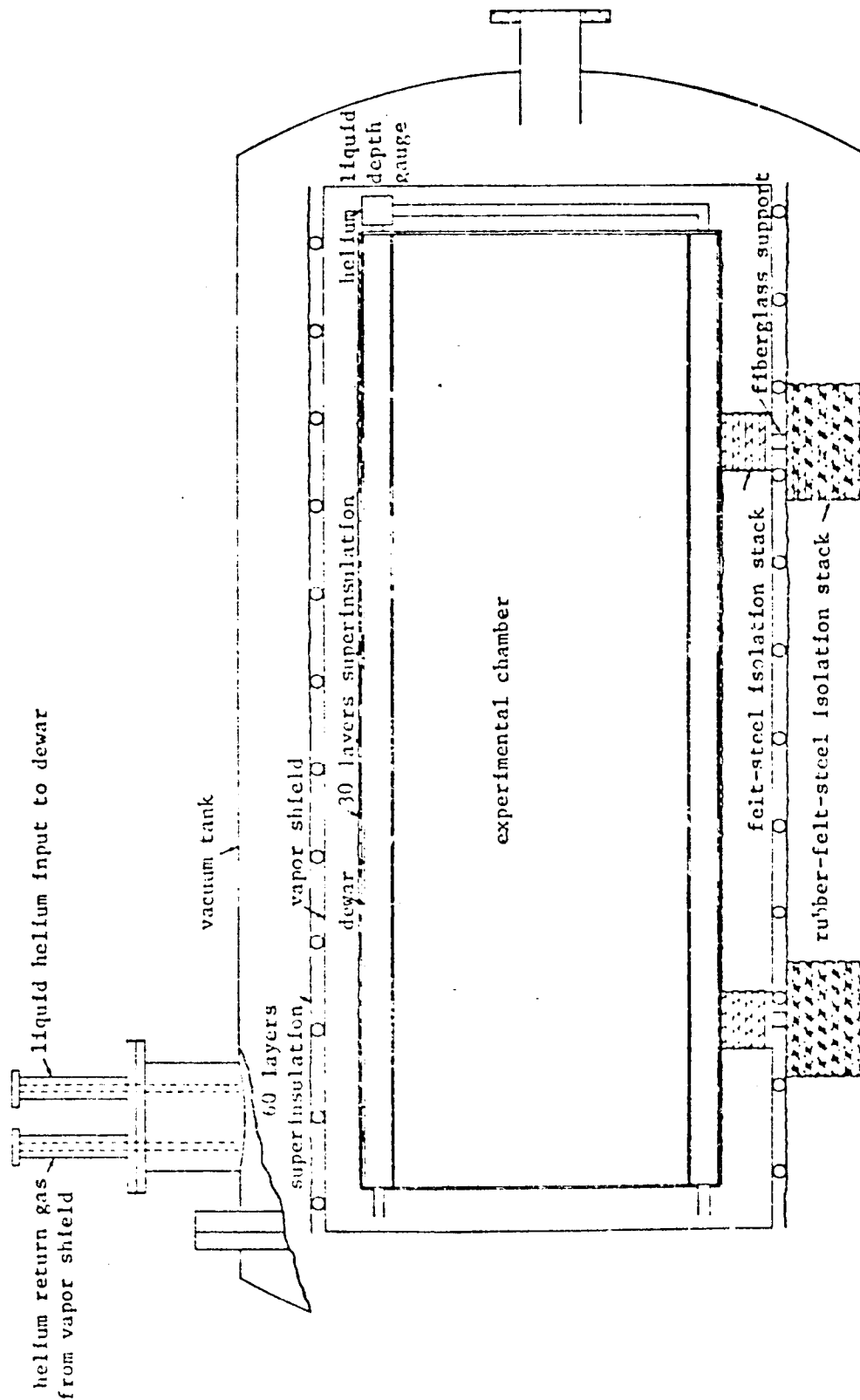


Figure 6. The Cryostat, cross section, side view

#### E. Temperature Measurement and Control

Two resistance thermometers were used in this experiment. One was a germanium thermistor manufactured by Keystone Carbon Company, model L0904-100K-HE-T2. The calibration of this device was not very good. There were only two resistance measurements from the manufacturer, at 4 and 20 Kelvin. A typical resistance versus temperature graph for this type of device was also supplied. This was the same germanium resistor used in the previous experiments.

The second device was a carbon glass resistor manufactured by Lake Shore Cryotronics Inc., model CGR-1-10,000. The manufacturer also provided an accurate calibration over a wide range. This device was employed for the first time in this experiment.

The two resistance thermometers were mounted together on the base of the suspension assembly, so that the carbon glass device could be used to calibrate the germanium device. In this way the temperature measurements of previous experiments could be updated with a more accurate calibration.

Two different devices were employed to measure the resistance of the thermometers. They were both constructed here. The first consisted of a 4 hz resistance bridge, differential amplifier, tuned amplifier, and phase sensitive detector. The bridge was balanced in the usual way by nulling the output signal. These electronics were used almost exclusively with the germanium resistor.

The second device applied a 10 hz current of known small amplitude to the current leads of the four terminal connections of the carbon glass resistor. The voltage drop across the resistor was measured to provide the resistance.

It is important that the currents going through the resistance thermometers do not significantly heat them. This can be easily verified by increasing these currents by a factor of two and observing whether or not the resistance reading



changes. In both cases above they did not. The maximum power generated in the germanium resistance thermometer by the bridge electronics was  $10^{-9}$  watts. That for the electronics of the carbon glass resistor was  $10^{-12}$  watts.

The two resistance thermometers were mounted on the aluminum base of the suspension system of the crystal. Attached to the same base was a frame on which the aluminum thermal radiation shield was mounted. The latter completely surrounded the crystal as shown in figure 2. It was covered with five layers of "superinsulation" (aluminized mylar and nylon net).

Epoxied into the base were the heater resistors used to control the temperature. Control was accomplished by applying a voltage to these resistors to bring the temperature up to the desired value and then by varying this voltage to maintain the desired temperature. Figure 7 shows how this was done with the bridge and the germanium resistor. The integrator shown maintained the voltage across the heater at the level to keep the bridge at a null. Any changes in the germanium resistance (i.e. change in temperature) would offset the bridge causing the integrator to increase or decrease the power produced by the heater until the bridge was renulled. A similar control was also accomplished with the carbon glass resistor and its electronics. This technique worked well at keeping the temperature constant at one point, the point where the resistance thermometer was located. However as the liquid level in the dewar decreased, thermal gradients inside the experiment chamber changed. Thus the temperature at other points changed. The change in the average temperature of the crystal during temperature control was measured by measuring the frequency of the crystal. Changes in this frequency were then related to changes in temperature. Thus the rate at which the crystal temperature was changing during those periods of temperature control was determined. Table I shows the results of these measurements. Also shown in

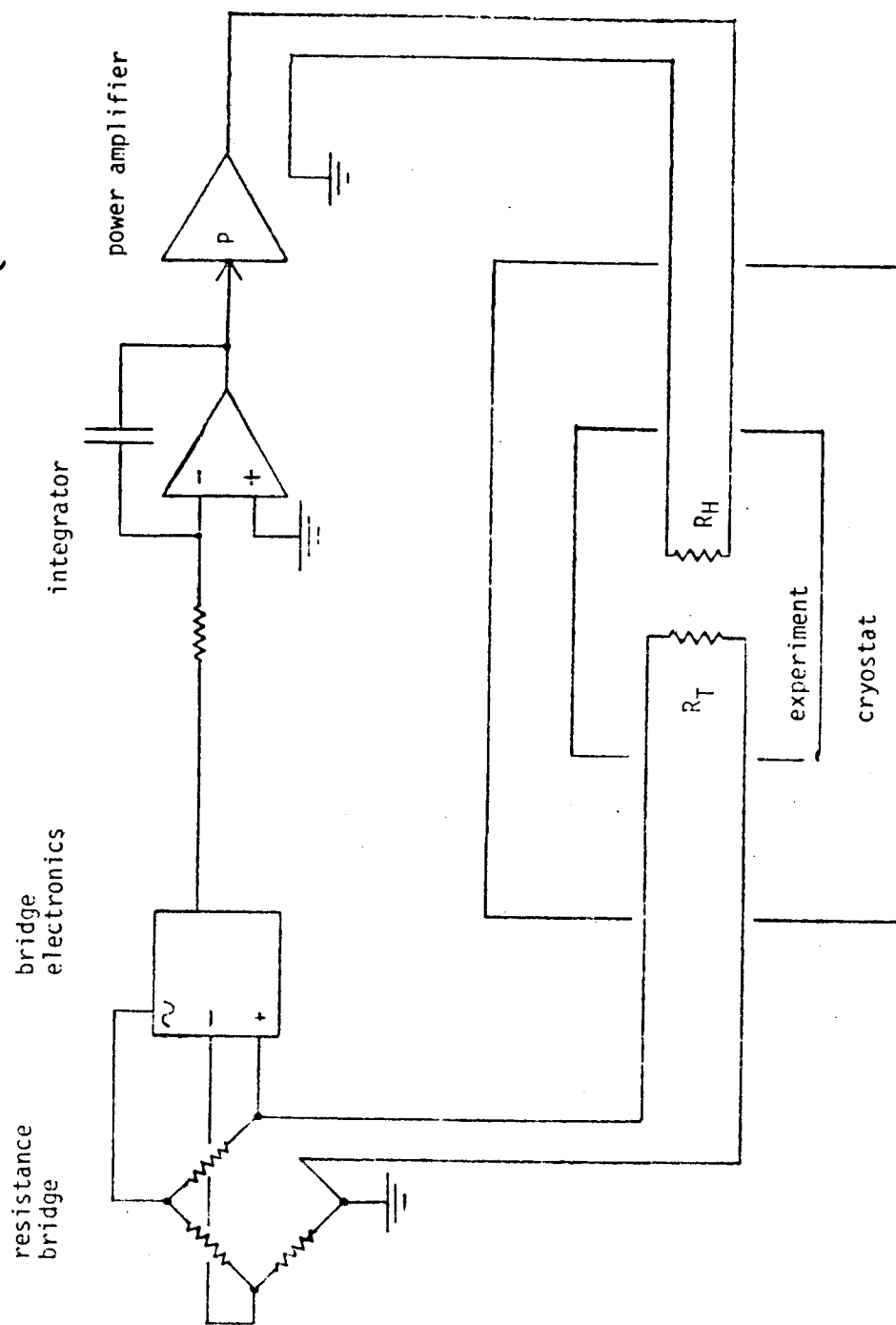


Figure 7. Temperature Control Feedback Loop  
 $R_T$  is the resistance thermometer  
 $R_H$  is the heater resistor.

Table I. Temperature Drift During Q Measurements

	Oct/Nov 79 Without temp. control	May/June 80 With temp. control
5K	.4 K/day	5.12K .05 K/day
7K	4 K/day	6.80K .3 K/day
11K	10 K/day	11.0K <.4 K/day
12K	9 K/day	12.1K <.6 K/day
14K	3 K/day	14.1K < 1 K/day

this table is the temperature drift from the previous experiment without temperature control. As seen from this data the drift with control was mostly a factor of ten less than that without control.

## RESULTS OF Q MEASUREMENTS

The graph in figure 8 shows the results of the two most recent Q measurements of the silicon crystal below twenty Kelvin. The 1979 measurements were made while the crystal was warming up. This data is similar to that of the previous experiments. The 1980 measurements were made with active temperature control of the crystal. This resulted in a temperature drift which was a factor of ten lower than the previous measurements as discussed in section II E. One purpose of this experiment was to compare the shapes of the Q curves with and without temperature control. It can be seen from the figure that the difference is quite significant. It is so markedly different in fact that it leads one to consider the possibility that factors other than temperature control could have produced it. These other factors will be discussed next.

Both experiments used the same four point suspension and transducer, i.e. that shown in figure 1 and discussed in section II A. Beneath the suspension were aluminum spacers. These were different in the experiments. The base to which the suspension and spacers were attached was also different. For the 1979 experiment without temperature control the base was a thirteen pound block of steel. For the 1980 experiment with temperature control the base was an eight pound aluminum block and frame for the thermal shield (figure 2). It is not yet known if this difference is significant.

There are other factors which may potentially affect the Q. Each time the crystal is set upon the four point suspension and allowed to rock back and forth (as happens when the bar assembly is slid into the cryostat), a small amount of aluminum rubs off and is embedded on the surface of the

ORIGINAL PAGE IS  
OF POOR QUALITY

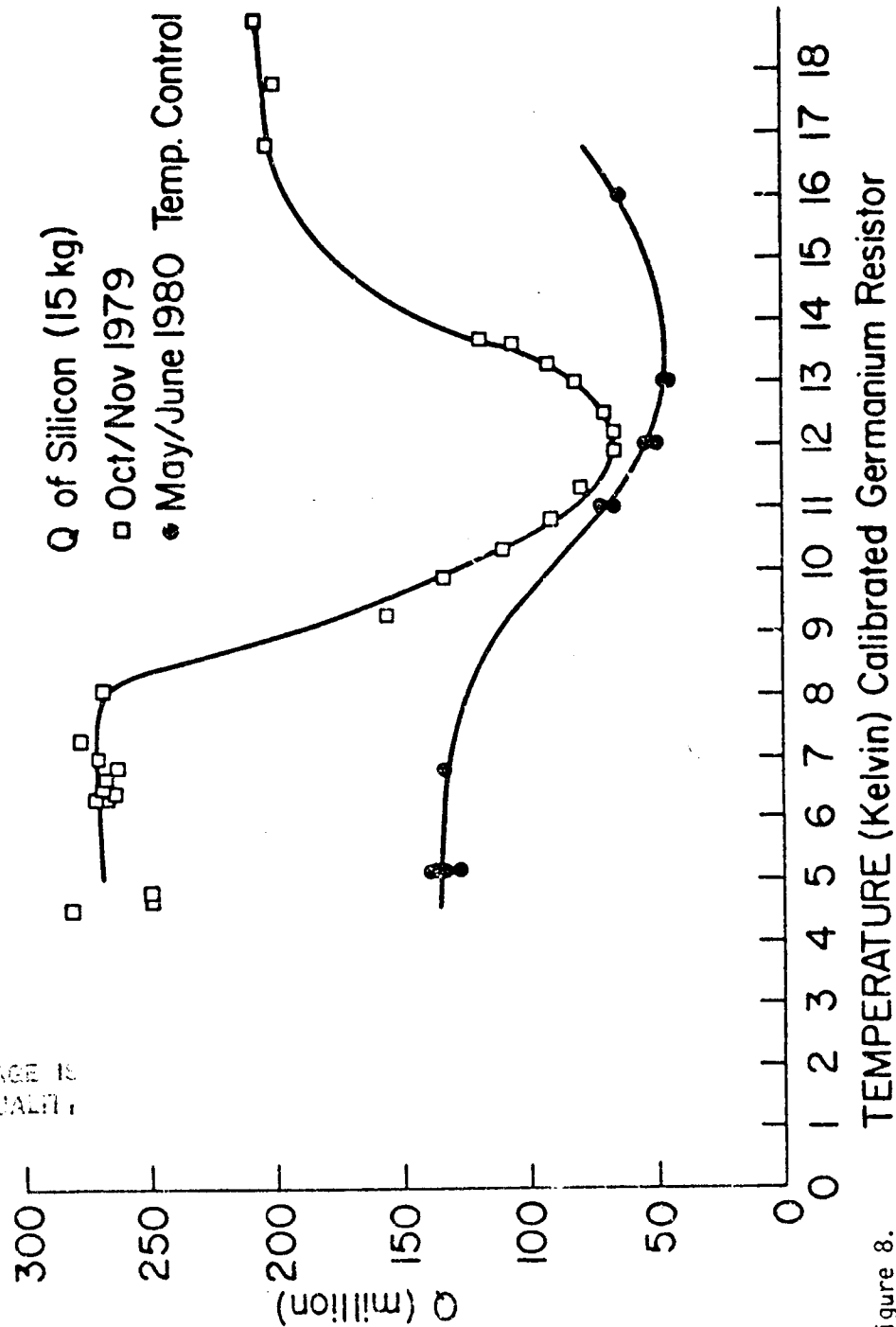


Figure 8.

crystal. This is visible on the surface. The aluminum builds up continuously. No attempt has yet been made to clean off the build up. It is possible that this produces a degraded Q after successive runs. The highest Q obtained was on the first run of the Q measurements ( $Q = 320 \times 10^6$ , 1978). The highest Q obtained during the 1979 and 1980 runs was  $280 \times 10^6$  and  $140 \times 10^6$  respectively. Thus the Q appears to be getting smaller. This could be caused by the aluminum or by some other accumulating damage to the crystal.

After warmup to room temperature of the last experiment, careful observations were made to determine if anything was touching the bar other than the suspension. Nothing was observed. Further experimentation at room temperature was done with the suspension and base to see the effect on the Q. Table II is a summary of these observations and also includes previous room temperature Q measurements. The 1978 measurements were made before the first cooldown of the silicon, the 1980 measurements were made before the last cooldown, and the 1981 measurements were made after the last cooldown. The last two measurements used a different four point suspension and transducer. This different suspension is shown in figure 9. The transducer was a piezoelectric ceramic glued on the surface of the crystal with GE 7031 varnish. From the data presented in this table the overall conclusion is that the room temperature Q is not strongly dependent on the base, suspension, and transducer configurations which were tested.

Table II. 300 K Q Measurements

Date	Suspension	Transducer	Base	Q (10 <sup>6</sup> )
3-23-78	center ring*	pzt on suspension	13 lb. steel	67
4-24-78	center ring	pzt on suspension	13 lb. steel	80
8-6-80	center ring	pzt on suspension	8 lb. aluminum	63
8-7-80	center ring	pzt on suspension	8 lb. aluminum	68
1-7-81	center ring	pzt on suspension	8 lb. aluminum	54
1-12-81	four arm*	pzt on crystal	8 lb. aluminum	63
2-9-81	four arm	pzt on crystal	13 lb. steel	59

\* The "center ring" suspension is shown in figure 1.

The "four arm" suspension is shown in figure 9.



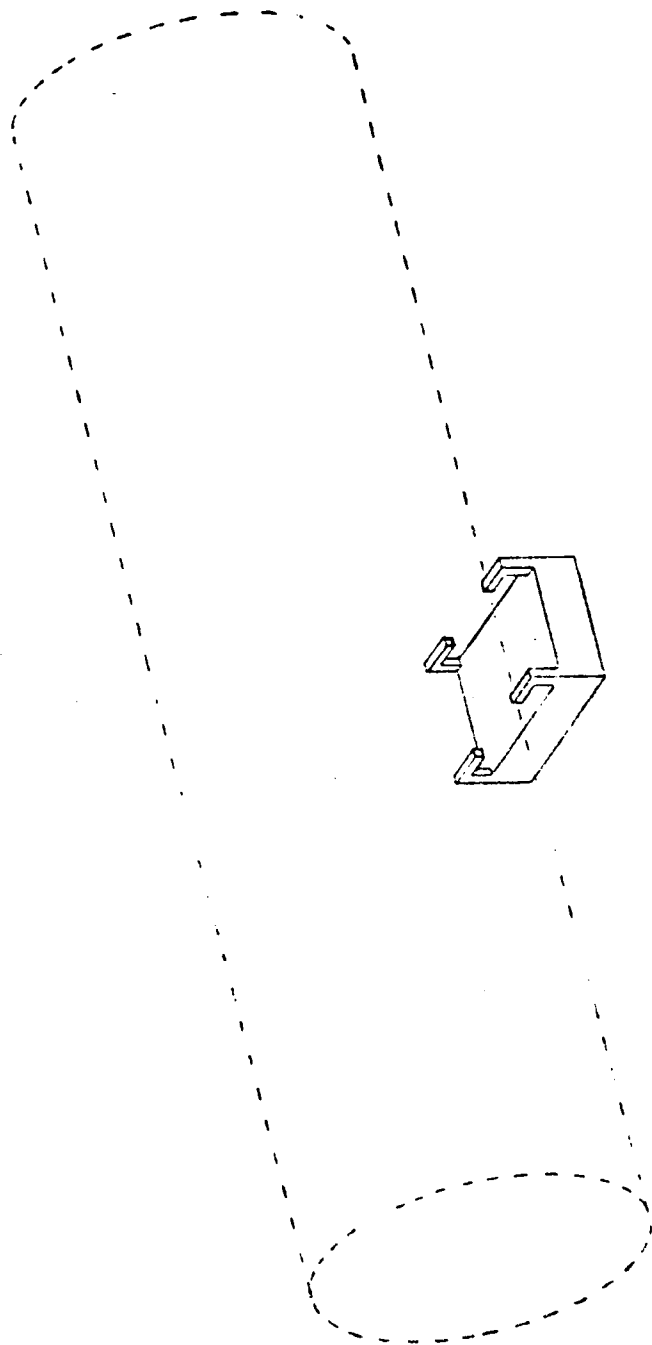


Figure 9. "Four Arm" Suspension

## RESULTS OF FREQUENCY MEASUREMENTS

The graph of figure 10 shows the frequency of the fundamental mode of the silicon crystal as a function of temperature below 18 Kelvin. These data are for two separate experimental runs, one with and one without temperature control. Data for temperatures above 18 Kelvin are given in the previous report. The important characteristic of the latter data is that as the temperature increases the resonant frequency decreases, i.e.  $df/dT$  is negative above 18 Kelvin. The data in figure 10 show the frequency increasing from 5 to 15 Kelvin, then sharply decreasing above 17 Kelvin. The derivative  $df/dT$  equals zero somewhere in the range from 15 to 17 Kelvin. Above that range it is negative, below it is positive. As pointed out by the previous report the data published by a group at the University of Rochester <sup>1</sup> gives frequency (as well as Q) measurements of a silicon crystal down to 4 Kelvin. These data show  $df/dT$  to be negative in the entire range from 4 to 300 Kelvin. It is not clear why this difference exists. See the previous report for a comparison of the experiments.

The frequency of the silicon crystal can be related to its coefficient of thermal expansion. Data published by Lyon, Salinger, and Swenson <sup>2</sup> give the coefficient of thermal expansion of silicon down to 6 Kelvin. It is positive from 6 Kelvin to 18 Kelvin and negative from 18 to 120 Kelvin. More study of the relation between the resonant frequency and the thermal expansion is indicated by these data.

---

<sup>1</sup> McGuigan, D. F., Lam, C. C., Gram, R. Q., Hoffman, A. W., and Douglass, D. H., "Measurements of the Mechanical Q of Single-Crystal Silicon at Low Temperatures," J. of Low Temp. Phys., 30, 621 (1978).

<sup>2</sup> Lyon, K. G., Salinger, G. L., and Swenson, C. A., "Linear thermal expansion measurements on silicon from 6 to 340K," J. of Applied Physics, 48, 865 (1977).

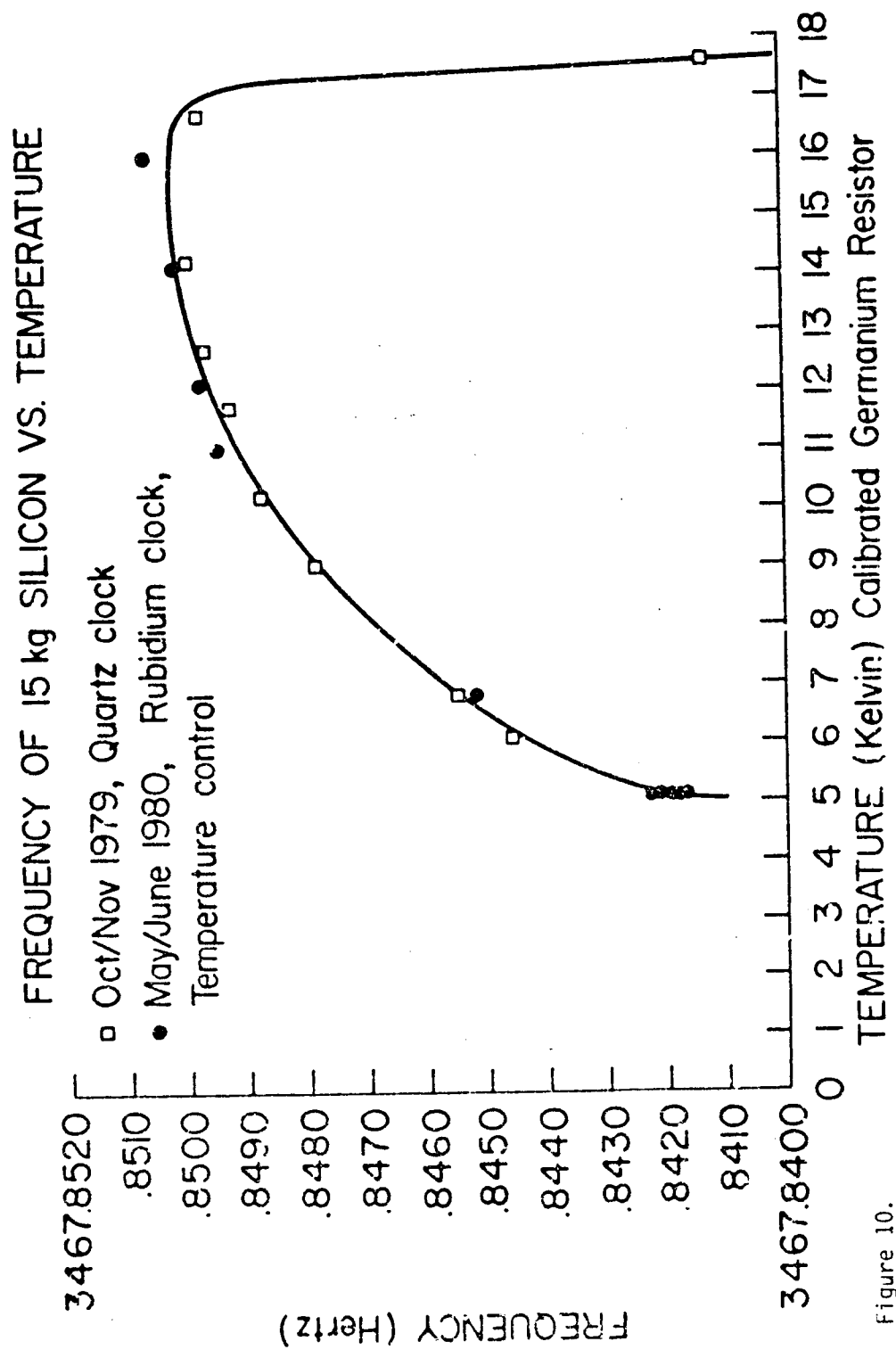


Figure 10.

## PART II: CRYSTAL EXPERIMENTS AT $T < 4K$ .

### INTRODUCTION

The study of the properties of single crystal silicon and sapphire by our group at the University of Maryland has indicated that temperatures below that of liquid helium are needed in order to more thoroughly understand the mechanisms of acoustic loss in these crystals. Toward this objective, we have recently acquired a  $He^3 - He^4$  dilution refrigerator from the S.H.E. Corporation. This device will allow us to reach temperatures of approximately .02 K. The dilution refrigerator is described in Appendix I. Because of the size of the crystals under study, however, a fairly large volume would have to be cooled. This necessitated the construction of a liquid helium cryostat of a size and configuration unavailable commercially. This cryostat is described in Appendix II. The following is an explanation of the experiments that will be conducted at  $T < 4K$ .

## PROPOSED EXPERIMENTS

We are presently planning to measure the mechanical Q's of several materials at temperatures down to 20 milliKelvin and possibly below. The outline on the following page and the illustration of figure 11 summarize the proposed experiments. They are to be cooled with the SHE Model 420 helium dilution refrigerator and Maryland built cryostat described in this report.

The materials will be in the form of bars each about seven inches long and two inches in diameter. Two different types of suspensions are to be used. The first is a four point rigid aluminum suspension shown in figure 12. This type of suspension has been successfully used at 4 Kelvin to obtain Q's of up to  $4 \times 10^8$ . With bars of potentially higher Q this type of suspension is expected to be a limiting factor. Other materials with higher Q than aluminum alloy 6061 might be used to construct the rigid suspension, but ultimately we expect the necessity of using magnetic levitation.

The transducer excites one of the longitudinal normal modes of the crystal, usually the fundamental mode. Once excited, the crystal "rings" for a long time. While the crystal is ringing, the same or another transducer is used to generate an electronic signal from the mechanical oscillation. This signal is then amplified and recorded as a function of time. From this recording, decay time constants and Q's are calculated. The DC biased capacitor transducer (see figure 13) has been used successfully at 4 Kelvin and will be used initially for the proposed milliKelvin experiments. From a noise standpoint, the FET amplifier is best matched to the capacitor transducer. However, to observe crystal oscillations at lower amplitudes a quieter

amplifier and transducer combination is required. Such a combination is the RF biased SQUID amplifier coupled to flat coils with a persistent current as shown in figure 14. The flat coil magnetic transducer is especially suited to be used with magnetic levitation, because it can double as horizontal stabilization coils.

The initial millikelvin experiment will contain a niobium and an aluminum bar. The silicon and sapphire bars are not presently available, for they are now being coated with niobium. However, knowledge of the Q of niobium and aluminum is important for the crystal experiments, since niobium is the crystal coating and aluminum will support the crystals initially. Ultimately we wish to measure at millikelvin temperatures the Q of niobium coated silicon and sapphire monocrystals, supported with magnetic levitation, and observed with magnetic (flat coil) transducer and SQUID amplifier.

## Outline of Proposed Experiments

- I. Q measurements of materials down to 20 mK.
  
- II. Materials to be tested
  - A. Aluminum alloy 6061
  - B. Niobium
  - C. Silicon coated with niobium
  - D. Sapphire coated with niobium
  
- III. Suspension, transducer, and amplifier
  - A. Presently used system for testing each of the above materials
    - 1. Aluminum four point suspension
    - 2. DC biased capacitor transducer
    - 3. FET amplifier
  
  - B. Advanced system for testing each of the above materials except aluminum
    - 1. Magnetic levitation suspension
    - 2. Flat coil transducer with persistent current
    - 3. RF biased SQUID amplifier

## MAGNETIC LEVITATION

In order to isolate the crystals under investigation as much as possible, they will be magnetically levitated. This is accomplished by coating the bars with a thin layer of niobium. When the niobium goes superconducting it excludes any magnetic fields from the interior of the bar. This creates a magnetic pressure given approximately by  $p = \frac{B^2}{2\mu_0}$  (all units in MKS). This pressure is exerted against the bar and, if the field is properly shaped, will "float" the bar. (The proper way to calculate the necessary field strength is to recognize that the magnetic field must vanish at the superconducting boundary and solve the resulting image problem; however, the above equation serves as a first approximation.) If we consider a silicon bar, 7 inches by 2 inches diameter, the necessary magnetic field strength to levitate is  $\sim 500$  gauss. The first critical field of niobium is 1980 gauss at  $T = 0$  and  $\sim 1600$  gauss at  $T = 4.2\text{K}$ . Since the applied field is below the first critical field, the London equation can be used to calculate the penetration depth of the magnetic field and therefore the thickness of the niobium coating needed. The London equation states that the magnetic field varies exponentially with distance into the superconductor with characteristic length  $\lambda_L$  called the London penetration depth. This penetration depth must be modified when  $\lambda \ll \xi_0$ .  $\lambda$  is the mean free path length of the normal electrons, and  $\xi_0$  is the coherence length of the superconducting electrons. The penetration depth becomes  $\lambda \sim \lambda_L \left( \frac{\xi_0}{\lambda} \right)^{1/2}$ . Since at low temperatures electron scattering is dominated by lattice imperfections and impurities, the worse case for niobium would be  $\lambda = 3.3\text{\AA}$ , which is the lattice spacing. With  $\lambda_L = 390\text{\AA}$  and  $\xi_0 = 380\text{\AA}$  this gives  $\lambda = .4\mu\text{m}$ . Therefore, a coating  $\sim 1\mu\text{m}$  thick would be adequate.



The coating process will be a chemical vapor deposition. In this process a low melting point niobium compound is evaporated and allowed to come in contact with the crystal. The crystal has been heated so that the niobium compound dissociates on contact and pure niobium is deposited. This method was chosen over the more energetic sputtering or plasma spray techniques of deposition so as to minimize damage to the crystal. The resulting coating will be 5 - 20  $\mu\text{m}$  thick.

When a flux coil is near a superconducting surface, its inductance is a function of distance from the surface. To stabilize the bar in the direction parallel to the cylinder axis, two flat coils will be positioned at the ends of the bar. By measuring the ac component of the inductance of the coils we can instrument the bar. Since nothing will be touching the crystals except a thin layer of niobium, we expect to get good isolation.

A drawing of the magnetic levitation coil for small monocrystals is shown in figure 15.

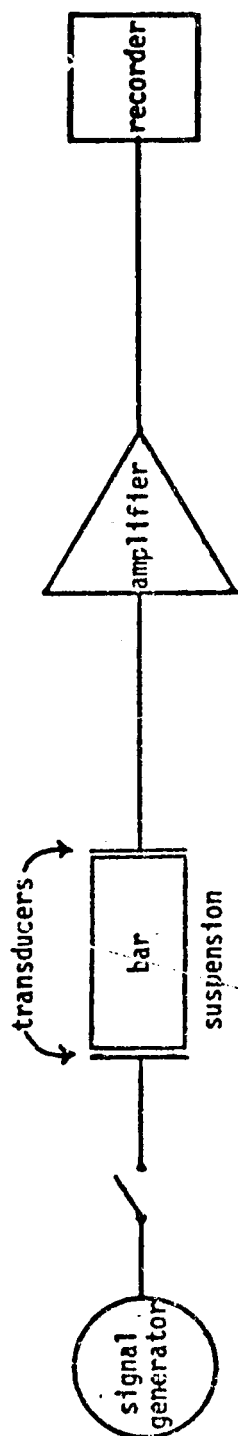


Figure 11. Simplified illustration of proposed experiments

ORIGINAL PAGE IS  
OF PAGES 177

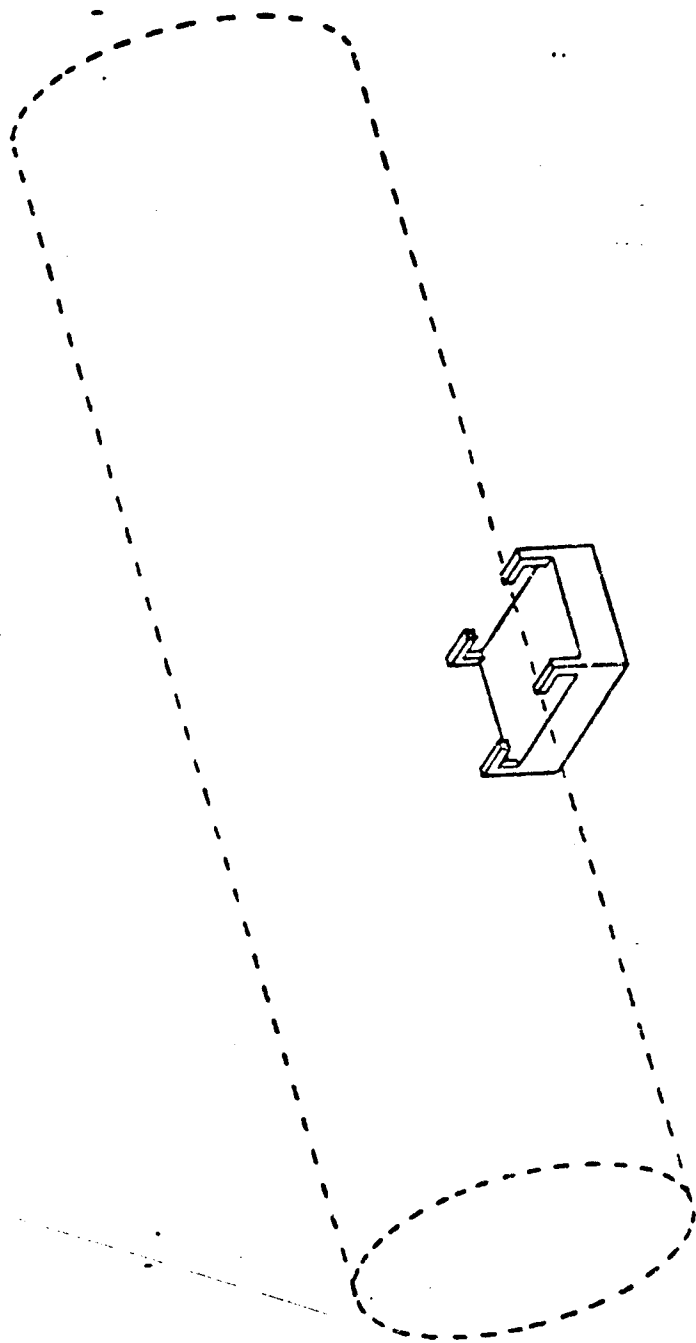


Figure 12. Four point rigid suspension

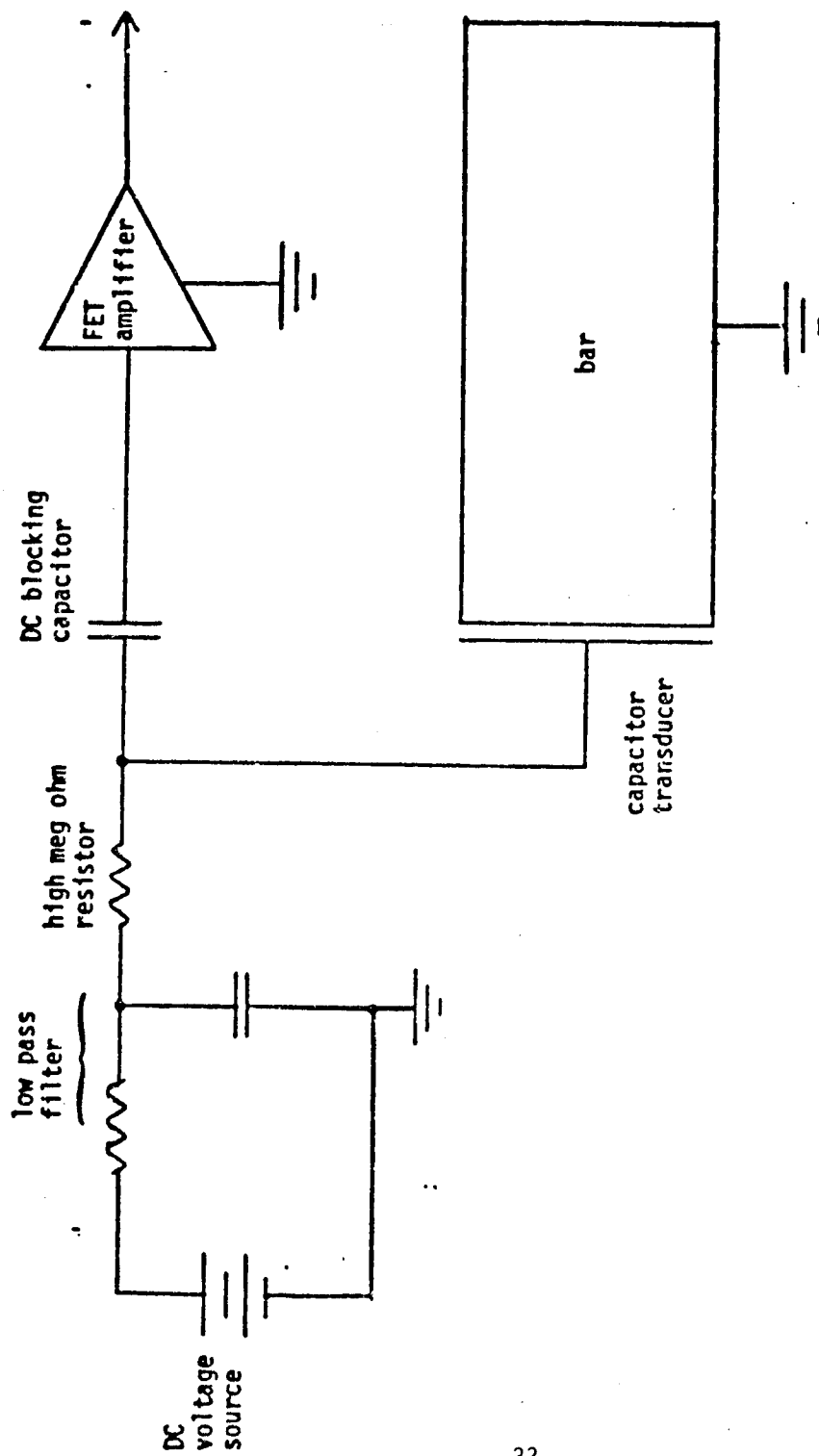


Figure 13. DC biased capacitor transducer

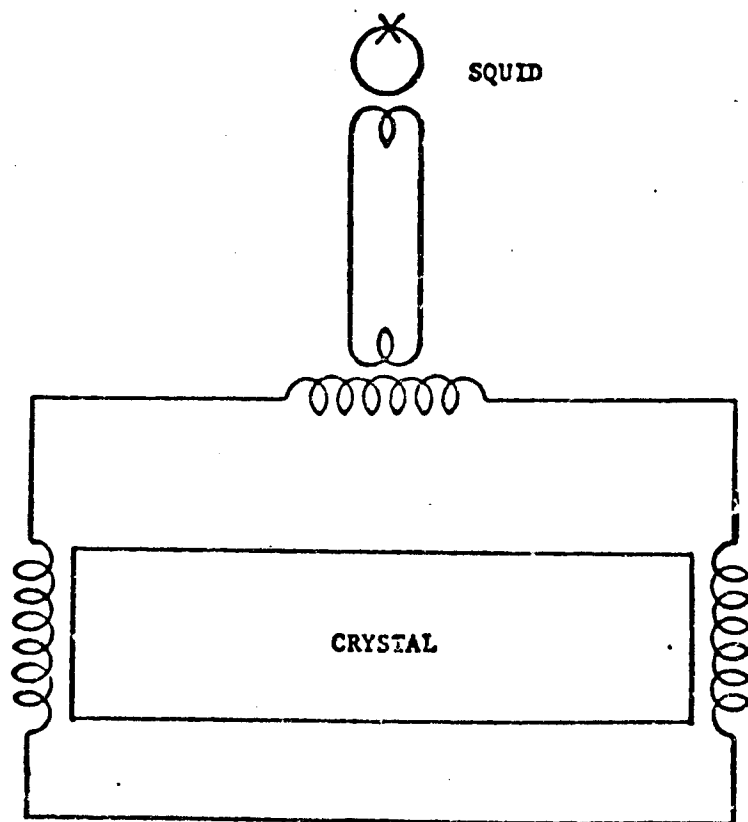


Figure 14. Superconducting Inductive Pickup

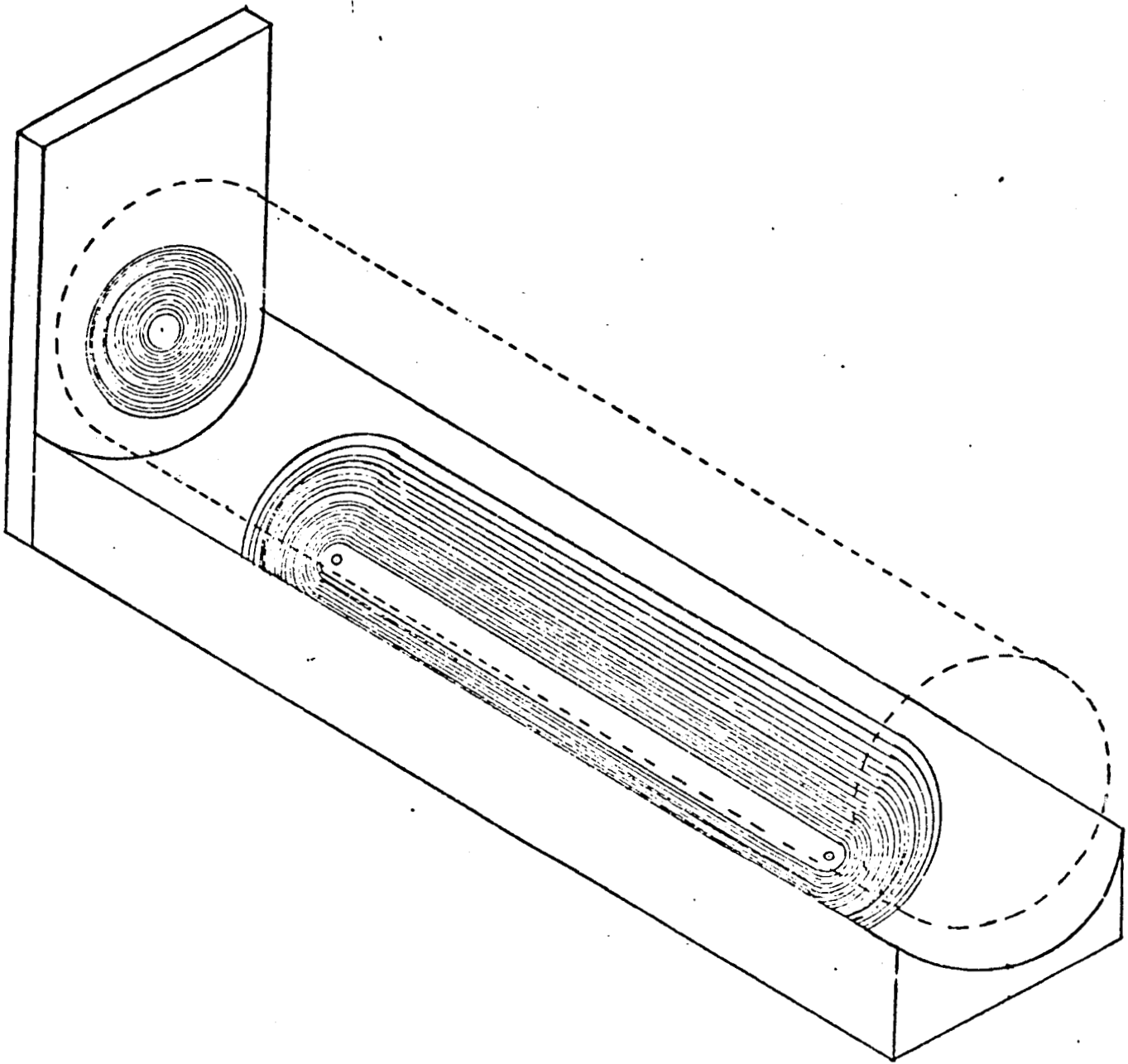


Figure 15. Magnetic levitation coil design

Appendix I

Description of The  
S.H.E. Corporation Dilution  
Refrigerator.



SHE CORPORATION

## SERIES 400 DILUTION REFRIGERATORS

### FEATURES

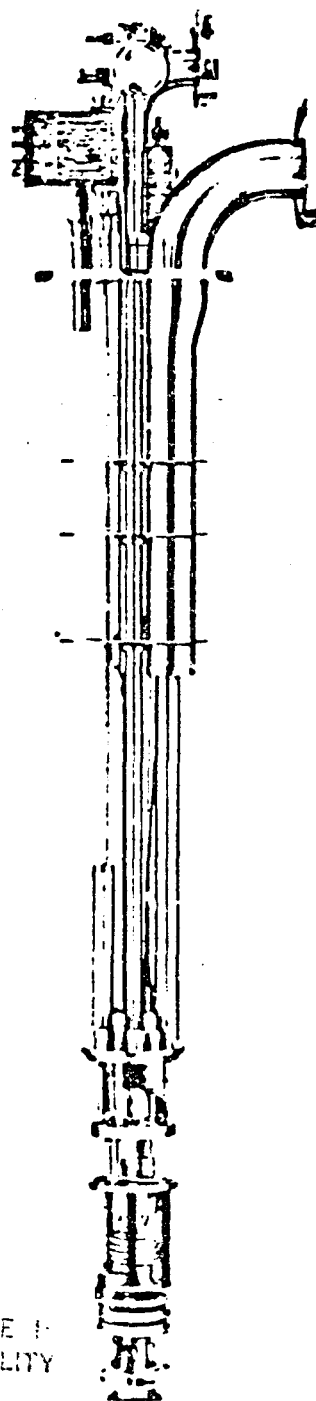
- Lowest Minimum Temperature
- Largest Cooling Powers
- Rugged, Convenient Construction

### INTRODUCTION

SHE's Series 400 dilution refrigerators represent new designs based upon recent fundamental advances in dilution refrigerator technology. Sintered silver heat exchangers have been incorporated into improved cryostat insert designs to provide superior performance and maximum reliability. Four, high-performance Series 400 cryostat inserts are presently available; every aspect of their design reflects the years of dilution refrigerator experience found only at SHE.

All Series 400 cryostat inserts have the following features:

- Metal surfaces of the dilution unit are gold-plated to improve thermal contact and prevent corrosion.
- Low temperature components of the refrigerator are supported by graphite-filled polyimide rods which provide excellent thermal isolation and are virtually unbreakable.
- Long-term reliability is ensured by repeated thermal cycling and leak testing of every joint. All pumping lines and flanges are of welded, stainless steel construction to avoid the need for possibly corrosive fluxes.
- A continuously operating coldplate condenses the incoming  $^3\text{He}$  and provides spare cooling power to thermally ground large heat loads at 1.3 K. This allows continuous operation of the dilution refrigerator at its minimum temperature, even when transferring helium into the dewar.
- Spare access ports located on the top-plate, vacuum flange, and coldplate facilitate future installation of special purpose leads, capillaries, coaxes, pumping lines, or other accessories. Two ports are vertically aligned from the top-plate through to the still.
- The standard copper mixing chamber has provision for both internal and external sample mounting. External samples are bolted to a heavy, gold-plated mounting flange; excellent thermal contact to the liquid helium inside the mixing chamber is established by a large quantity of sintered metal.



ORIGINAL PAGE 1  
OF POOR QUALITY

Model 420 DRI



Under typical operating conditions, the temperature difference between the inside and outside is less than 1 mK. Even when operating with the maximum possible external heat load, the difference is less than 3 mK at all temperatures.

- Radiation baffles on the pumping tubes (used to decrease helium boil-off in the dewar) are screwed in place, allowing for easy removal and modification.
- A heavy, 0.6 K thermal shield is attached to the still and surrounds the mixing chamber and experimental region.
- Carbon resistance thermometers are located on the coldplate, still, baseplate, coldest heat exchanger, and the mixing chamber for monitoring the refrigerator's performance. Heaters are installed on the coldplate, still, and mixing chamber. These heaters and thermometers utilize only 14 of the 24 shielded, low-frequency leads which are standard, leaving 10 for other applications.
- A unique sintered metal heat exchanger on the baseplate, below the continuous heat exchanger, has a large cooling power for thermal grounding at 50 mK.

The final step in the production of each SHE cryostat insert is a complete performance test in our factory. It is cooled to its minimum temperature and then operated with various heat loads and circulation rates. Complete test data, along with a detailed installation and operation manual, is supplied with each refrigerator.

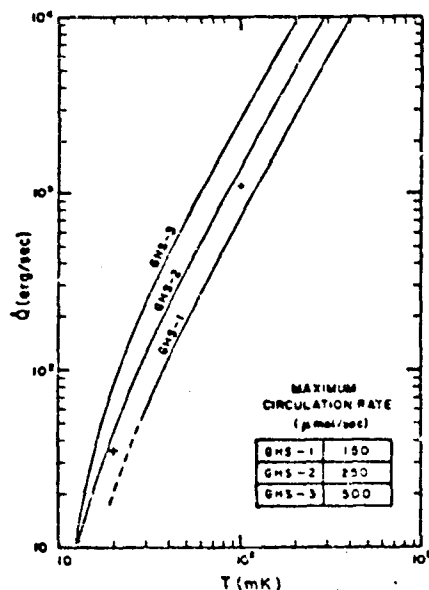


Fig. 2 Typical cooling power curves for Model 420 cryostat insert/gas handling system combinations. Some modification of the insert is required to accommodate the high circulation rates of the GHS-3. Points marked + indicate guaranteed minimum values with GHS-2. Minimum temperature is achieved with a circulation rate of 70  $\mu\text{mol/sec}$ .

## MODEL 420, GENERAL PURPOSE CRYOSTAT INSERT

The Model 420 is the smallest Series 400 Insert, yet its performance exceeds that of any refrigerator previously available. It has a typical minimum temperature of 6 mK and its cooling power, shown in Fig. 2, is far more than is usually required, even for demanding applications such as nuclear demagnetization or particle beam experiments.

The Model 420 is also the least expensive of the Series 400, both to purchase and operate. Only about six liters of liquid helium are required per day, even when operating at maximum circulation rates. It fits into a convenient 14-cm-diameter dewar neck, yet it has a large, 9-cm-diameter x 26-cm-long space below the mixing chamber for mounting experiments. Straight line, direct access from room temperature to the mixing chamber is provided down the vacuum can pumping line. This feature is unique to the Model 420 and requires only one vacuum feedthrough, at room temperature. The Model 420's superior performance, small size, and economical price make it the recommended cryostat insert for most applications.

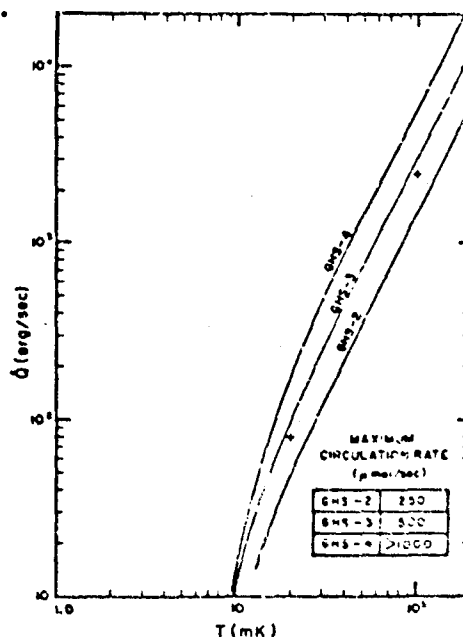


Fig. 3 Typical cooling power curves for Model 430 cryostat insert/gas handling system combinations. Cooling power achieved with GHS-4 represents that of the Model 430A. Points marked + indicate guaranteed minimum values with GHS-3. Minimum temperature is achieved with a circulation rate of 80  $\mu\text{mol/sec}$ .

## MODEL 430, HIGH-POWER CRYOSTAT INSERT

The next larger Series 400 cryostat insert, the Model 430, offers still better performance. It has a typical minimum temperature of 4.5 mK and its cooling power, shown in Fig. 3, is about double that of the Model 420. It is mechanically very strong and experimental packages weighing more than 10 kg may safely be mounted in the large, 14-cm-diameter x 63-cm space provided.

Several features are unique to the Model 430. These include two, parallel <sup>3</sup>He condensing systems which reduce the condensing pressure and help prevent blockage. Also provided is a flange, thermally grounded at 50 mK, to which an additional thermal shield can be attached for use with ultra-low temperature experiments. The bottom of the mixing chamber is sealed to the top by an indium O-ring so that it can be easily replaced with one of an alternate design. This provision can, for example, be used to allow very large experiments to be mounted inside the mixing chamber. Since the Model 430 requires larger pumps, and more liquid helium, it is generally recommended only for the most demanding applications.

## MODEL 430A, EXTRA-HIGH POWER CRYOSTAT INSERT

A modified version of the Model 430, the Model 430A, provides even higher cooling power (see Fig. 3). It is physically similar to the Model 430 and reaches the same minimum temperature, but its condensing system and still have been modified to allow larger circulation rates. It also has a unique, two-stage coldplate that supplies 60 mW of refrigeration for normal operation, or 120 mW when the refrigerator is operated at maximum circulation rate.

## MODEL 420-TL TOP-LOADING CRYOSTAT INSERT

The Model 420-TL is a modified version of the Model 420 cryostat insert that permits the operator to rapidly change samples without warming the entire refrigerator to room temperature. The samples are mounted on a special rod and inserted through an airlock on top of the cryostat into a tube leading down into the mixing chamber. Excellent thermal contact is established by immersing the sample in a liquid-helium-filled chamber attached to the mixing chamber. No mechanical clamps or screws are required. Cooldown time depends on the sample and its holder, but complete cycles from room temperature in much less than one hour are feasible. Electrical leads may be attached directly to the sample or the sample holder for measurements of electric, magnetic or thermometric properties. Even thermal conductivity and heat capacity measurements are possible using the quick-change sample loader.

## DILUTION UNITS

The dilution units (still, heat exchangers, and mixing chamber) of the Models 420 and 430 are available separately. The dilution unit for the Model 430 is shown in Fig. 4. These units are completely tested at SHE to ensure that the performance exceeds the guarantees of the complete cryostat insert. This performance requires adequate pumping speed and careful installation to eliminate heat input due to thermal radiation, vibration, rf heating, and other causes. For this reason it is not possible to guarantee that the full performance capability will be achieved by the user when only the dilution unit is purchased.



Fig. 4. DRP 430

## SPECIFICATIONS

	Model	
	Model 420	430, 430A
Minimum Temperature	Typical:	6 mK
	Guaranteed:	4.5 mK
Cooling Power	Typical:	8 mK
	Guaranteed:	7 mK
Helium Charge, includes normal room temperature volumes	See Fig. 2	See Fig. 3
	<sup>3</sup> He 0.6 mol	<sup>3</sup> He 1.2 mol
Dimensions (cm)	<sup>3</sup> He 1.8 mol	<sup>3</sup> He 3.6 mol
	Overall length	182
Bottom of top-plate to bottom of vacuum can	146	185
	Maximum diameter below top-plate at battle	13.7
Experimental space below mixing chamber (cm)	Length	26.0
	Diameter	8.5
		63.5
		13.8

[illegible][illegible]

ORIGINAL PAGE IS  
OF POOR QUALITY

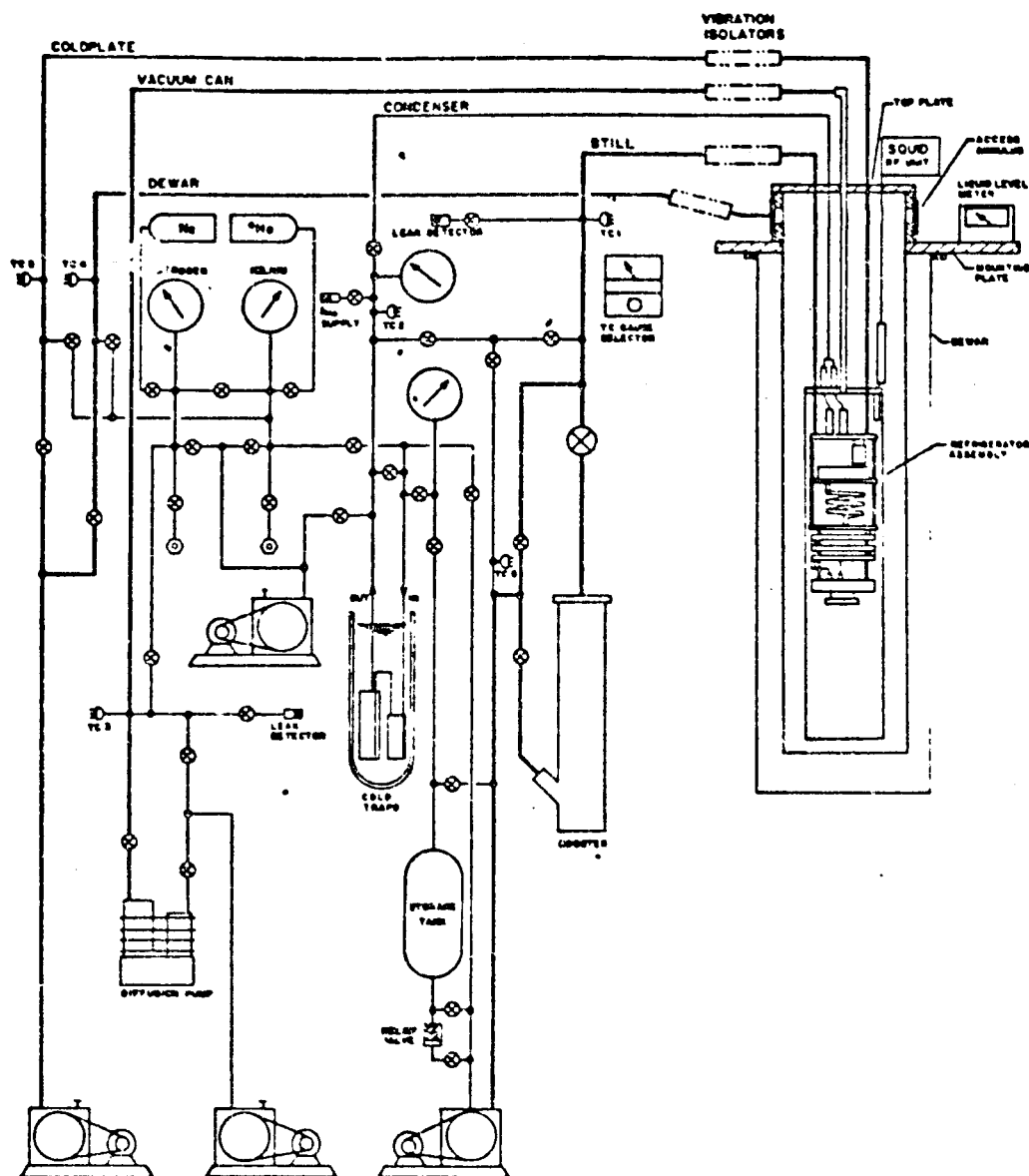


Fig. 2. Schematic Diagram of the Model GHS-3 Gas Handling System

TABLE 1 SHE Pumping and Gas Handling Systems

SYSTEM DESIGNATOR	VACUUM ISOLATION			10 COLDPLATE PUMPING		VACUUM CAN PUMPING		PUMP PURGE SUBSYSTEM	
	AP Necessary Valves & Pumping	Booster Pump	Booster Pump*	AP Necessary Valves & Pumping	10 sec Rotary Pump	AP Necessary Valves & Pumping	150 mm Rotary Pump	AP Necessary Valves & Pumping	150 mm Rotary Pump
F	X	X	X	X	X	X	X	X	X
H	X	X	X	O	O	O	O	O	O
F(NP)	X	X	X	X	O	X	O	X	O

X—Supplied with System

O—Customer must furnish

\*Supplied with the GHS-2, 3, and 4.



SHE CORPORATION

## PUMPING AND GAS HANDLING SYSTEMS

### FEATURES

ORIGINAL PRICE IS  
OF POOR QUALITY

- Convenient and easy-to-learn operation
- Highest quality components and construction throughout

A properly designed gas handling system is essential to the performance of a dilution refrigerator. Pumps, valves, and pumping lines must be carefully matched to achieve the refrigerator's full potential. It is equally important that it be easy to use, that it provide long-term vacuum integrity, and that it have adequate protection against power failure, cooling water shut-down, and circulation blockage. SHE Gas Handling Systems have all these features and come in a variety of models to provide a wide range of refrigeration capabilities.

Only the highest quality components and construction techniques are used throughout these systems. All valves and gauges are mounted on large aluminum panels which are bolted to a sturdy support frame. This eliminates motion of the components which could result in vacuum leaks. Vacuum sensors are employed in important parts of the circuit and are monitored on a meter mounted on the front panel of the system. A panel mounted switch allows the user to select between sensors. The panels feature a clear, full-sized diagram of the plumbing arrangement and all valves and gauges are integrated into this diagram to achieve the clearest possible exposition of the gas handling system, thereby minimizing the possibility of error in its use.

In order to provide maximum vibration isolation, SHE Gas Handling Systems are mounted physically separate from the cryostat insert and all interconnecting lines are supplied with special flexible sections. Additional flexible sections are used to further isolate the rotary pumps which are located behind the gas handling system.

Fig. 2 presents a diagram of the plumbing arrangement of a complete gas handling system. This system may be divided into four subsystems: the  $^3\text{He}/^4\text{He}$  subsystem, the 1 K refrigerator subsystem, the vacuum can subsystem and the pump/purge subsystem. Each of these is described in the following sections. Gas handling systems whose model designations end in "H" include only the  $^3\text{He}/^4\text{He}$  subsystem,

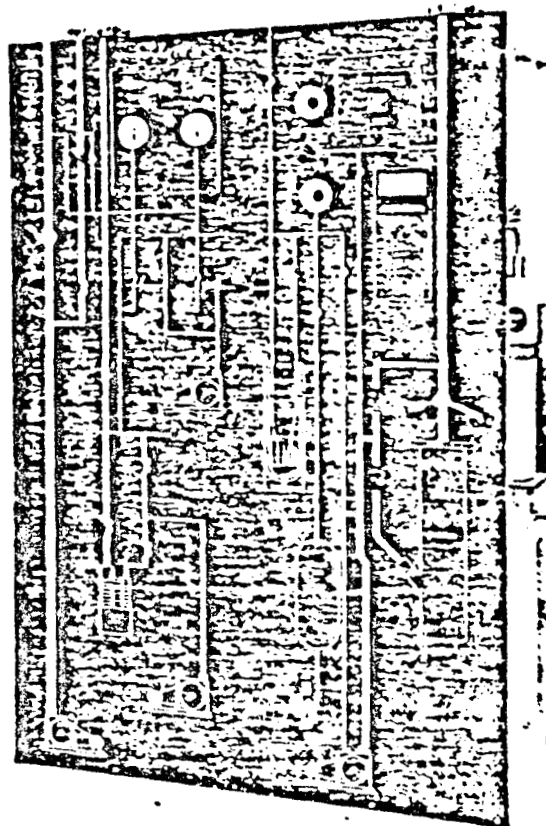


Fig. 1. SHE Model GHS-2F Pumping and Gas Handling System

tem, while those ending in "F" include all four subsystems. A gas handling system designated "F" with the additional suffix "NP" indicates a system provided with no rotary pumps except the sealed rotary pump in the  $^3\text{He}/^4\text{He}$  subsystem. See Table

### THE $^3\text{He}/^4\text{He}$ CIRCULATION SUBSYSTEM

The  $^3\text{He}/^4\text{He}$  subsystem includes a two-stage liquid nitrogen cooled trap, a storage tank, precision pressure gauges, and all pumps and valving needed to conveniently operate the refrigerator. Bypass valving is provided to throttle the circulation for stable operation at temperatures up to 2 K. This important feature ensures a substantial overlap of the operating range of a dilution refrigerator with that of a simple pumped helium bath. Provision is also made for connecti-

the subsystem via a precision metering valve to a mass spectrometer leak detector. This is useful for leak testing, measurement of the  $^3\text{He}$  content of the circulating gas and as an aid in diagnosing refrigerator performance.

A relief valve located in the subsystem shunts the  $^3\text{He}/^4\text{He}$  mixture into the storage tank in case a blockage of the refrigerator occurs, and allows unattended operation for extended periods. Valving is also provided to permit circulation of the mixture through the nitrogen-cooled traps prior to its admittance to the refrigerator, thereby ensuring that no contaminants reach the dilution unit.

Each gas handling system can be characterized by the pumps it employs and the circulation rate which can be achieved. The GHS-1 is supplied with a 10 l/sec rotary pump which, under typical operating conditions, provides circulation rates from 100-150  $\mu\text{mol}/\text{sec}$ . The GHS-2 and GHS-3 utilize oil vapor pumps as booster pumps with a 10 l/sec rotary pump to provide maximum circulation rates of approximately 250  $\mu\text{mol}/\text{sec}$  and 500  $\mu\text{mol}/\text{sec}$  respectively. The GHS-4 uses blower pumps to achieve circulation rates exceeding 2 mmol/sec.

## 1 K REFRIGERATOR SUBSYSTEM

This subsystem operates the continuous flow 1 K coldplate system and allows flow testing and purging of the coldplate during startup. In addition, a separately valved line branches from the main coldplate pumping line and connects to the helium space of the liquid helium dewar. This connection, together with a built-in interconnection to the pump/purge subsystem, enables one to flush both the coldplate system and the helium space of the dewar with helium or nitrogen gas during the startup and shut-down procedures. Separate vacuum sensors are provided for both the coldplate line and the dewar line.

## THE VACUUM CAN SUBSYSTEM

The vacuum space surrounding the dilution unit is evacuated by way of an oil diffusion pump, mounted in the gas handling system. Interconnection to the pump/purge subsystem is provided by way of a needle valve permitting one to flush the vacuum space during startup and to admit exchange gas to this space in a well-controlled fashion. A quick-connect fitting mounted on the side of the framework is provided to connect a mass spectrometer leak detector directly to the vacuum space.

## THE PUMP/PURGE SUBSYSTEM

This facility comprises a separate rotary pump, two compound retard pressure/vacuum gauges, a number of toggle vacuum valves, means to connect this subsystem to sources of nitrogen and helium gas, and hose connectors for attaching rubber tubing. This subsystem is connected to all other subsystems and allows the user to flush them with nitrogen or helium gas as needed. The hose connectors provide a convenient source of these gases for a variety of uses.

## INSTALLATION IN YOUR LABORATORY

All SHE gas handling systems come complete with large interconnecting pumping lines of negligible flow impedance. Separation of the cryostat support structure and gas handling system by a distance of two feet is standard, with additional separation available at extra cost. Fig. 3 gives the dimensions of the laboratory space required for the standard installation.

In order to maximize the vibration isolation between the gas handling system and cryostat insert, each SHE gas handling system is to be firmly bolted to the floor. In addition, provision is made to embed a short section of each pumping line in concrete between the main framework and the pump. Specially cut wooden forms are provided to allow one to pour this concrete block within the floor space occupied by the framework.

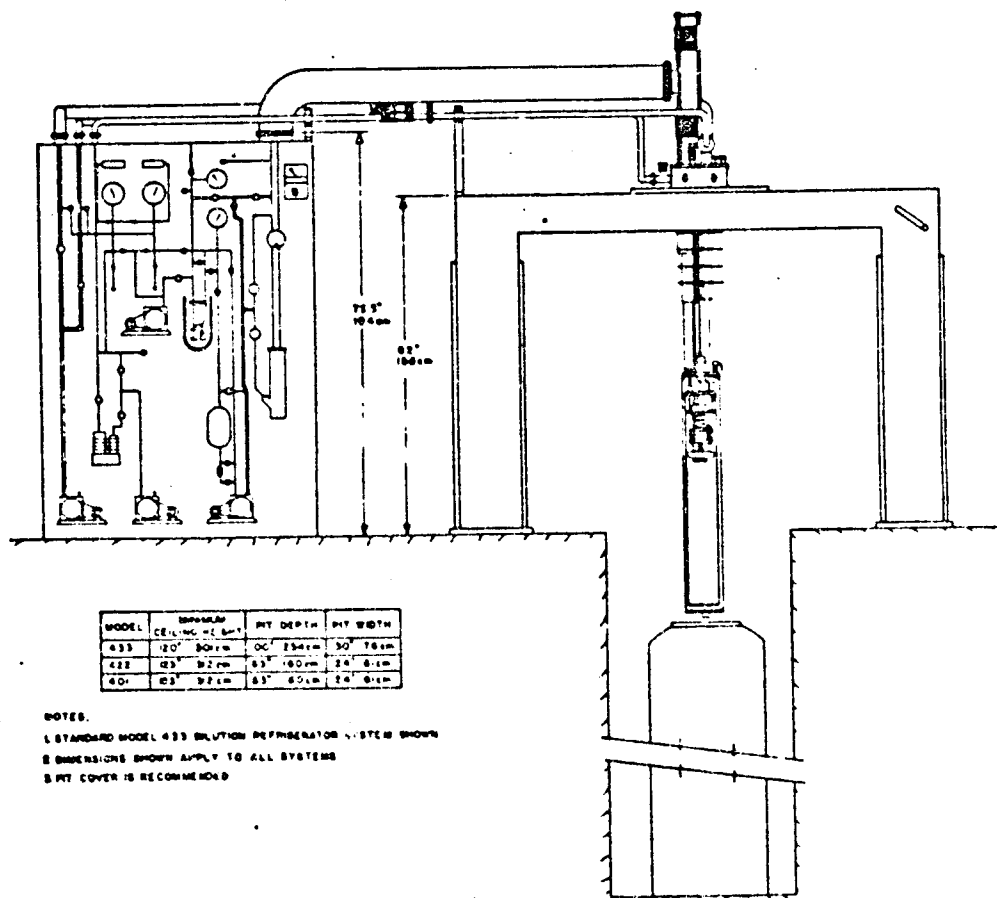
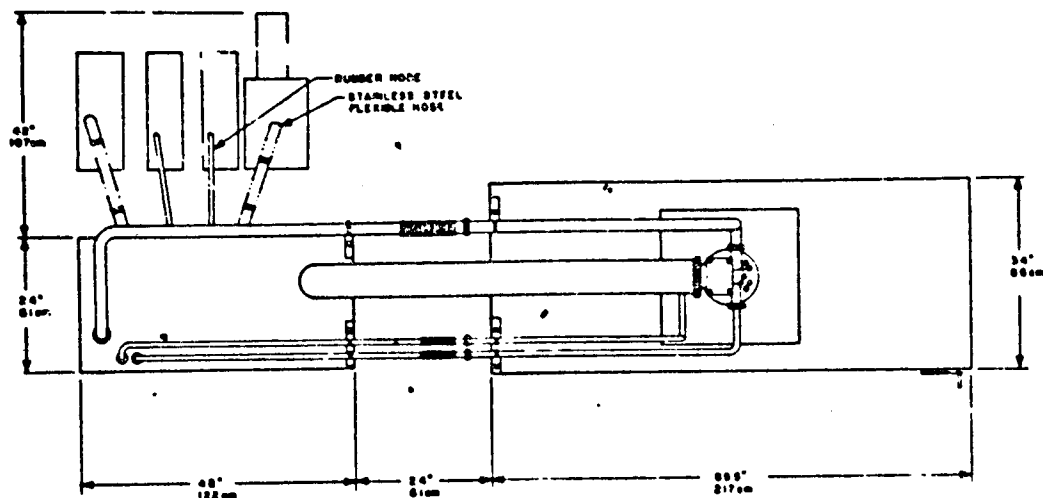
## OPTIONS

- Extra 35 or 100 liter storage tank with separate valving and gauge.
- Auxiliary valving allows use of pumps for another application such as evacuating the vacuum space of a helium dewar.
- Custom designed pumping lines—Longer lines, shorter lines, and special configurations, such as two-piece lines for use with an rf shielded enclosure, are available.
- Extra coldtrap—This option allows continuous operation of the refrigerator while cleaning contaminants from the regular coldtrap. All necessary valves and pumping lines are provided.

## SPECIFICATIONS

### $^3\text{He}/^4\text{He}$ Circulation Rate:

GHS-1	> 150 $\mu\text{mol}/\text{sec}$ , typical
GHS-2	250 $\mu\text{mol}/\text{sec}$ , maximum
GHS-3	500 $\mu\text{mol}/\text{sec}$ , maximum
GHS-4	> 2000 $\mu\text{mol}/\text{sec}$ , typical



MODEL	CEILING Ht. MIN.	PIT DEPTH	PIT WIDTH
433	120" 3048mm	60" 1524mm	30" 762mm
422	125" 3175mm	65" 1651mm	24" 610mm
401	125" 3175mm	65" 1651mm	24" 610mm

NOTES:

1. STANDARD MODEL 433 SOLUTION REFRIGERATOR SYSTEM SHOWN
2. DIMENSIONS SHOWN APPLY TO ALL SYSTEMS
3. PIT COVER IS RECOMMENDED

Fig. 3 Standard Installation—Model GHS-3

#### D-4. Performance Test

The assembled cryostat insert was given a complete low temperature performance test at SHE. It was mounted in one of the SHE in-house support structures and connected to the in-house gas handling system. An in-house liquid helium dewar was used for the test. Calibrated carbon resistance thermometers were installed on the coldplate, the still, the base plate, and the coldest heat exchanger. Most of these thermometers are from a special set used when testing, to allow more precise comparisons between refrigerators: thus these are not the resistance thermometers currently installed on the refrigerator. However, the coldest heat exchanger resistor currently installed is the same one used for the performance test. To measure the mixing chamber temperature, two CMN thermometer packages were installed; one was inserted through the bottom port on the mixing chamber to measure the temperature of the liquid helium inside the mixing chamber, and the other was fastened to the mixing chamber body to measure the temperature of the outside of the mixing chamber.

The thermometer packages use the Curie law dependence of the susceptibility of cerium magnesium nitrate, CMN. The packages contain an 11 mg CMN powder pill along with the excitation and detection coils for use with the SHE KLM measurement system. The RLM system measures changes in the mutual inductance between the excitation and detection coils; such changes are caused by changes in the susceptibility and hence the temperature of the CMN. The CMN thermometers were calibrated between 0.34 and 0.99 K using a calibrated germanium resistance thermometer installed on the outside of the mixing chamber. Liquid helium is used for thermal contact to the CMN. The external thermometer package was connected by a capillary tube to the dilute side of the coldest heat exchanger. The capillary let helium into the external thermometer package so that the CMN was in good thermal contact with its housing, which in turn was tightly bolted to the mixing chamber. The stub into which the capillary was soldered is still in place on the last heat exchanger: it may be unplugged and used for a similar purpose if desired.

The helium solution used in the dilution refrigerator system for the performance test contained 0.67 moles of  $^3\text{He}$  and 1.6 moles of  $^4\text{He}$ ; or in terms of liquid equivalent, 25 cm<sup>3</sup> of  $^3\text{He}$  and 45 cm<sup>3</sup> of  $^4\text{He}$ . The external CMN thermometer package contained about 1 cm<sup>3</sup> of  $^4\text{He}$ , and the adaptor piece used for the internal CMN thermometer added a volume of about 6 cm<sup>3</sup> of  $^4\text{He}$ . As indicated in Section 3-1, there is quite a large range for the acceptable quantities of both  $^3\text{He}$  and  $^4\text{He}$ .

Table D-1 shows the operating characteristics with no externally applied head load on the mixing chamber. The outside of the mixing chamber cooled to 6.5 mK, and the liquid helium inside the mixing chamber cooled below 6 mK. The independent variable for these data is the still power, determined by measuring the current through the still heater. The heater resistance is



TABLE U1

## Operating Characteristics - No Heat Load on Mixing Chamber

Dilution Refrigerator Model DRP-42, Serial No. 4232

$\dot{Q}_{\text{still}}$ mW	$\dot{n}$ $10^{-5} \frac{\text{mole}}{\text{sec}}$	Ratio $\frac{3}{4} \frac{\text{He}}{\text{H}_2}$	$\dot{n}_3$ $10^{-5} \frac{\text{mole}}{\text{sec}}$	Condensing Pressure torr	Temperatures					
					Cold Plate K	Still K	Base Plate mK	Coldest Heat Exchanger mK	Mixing Chamber* mK	
									INT	EXT
1.0	6.7	13.9	6.2	61	1.27	0.53	46	25	6.33	6.98
2.0	10.6	21.1	10.2	70	1.27	0.58	46	25	5.73	6.50
3.0	11.7	20.6	11.2	82	1.28	0.62	47	26	5.58	6.53
4.0	15.6	21.7	14.9	91	1.28	0.65	48	26	5.60	6.54
2.0 <sup>†</sup>	10.6	24.2	10.2	66	1.28	0.58	47	27	5.88	7.17

<sup>†</sup>This 2mW still power point was taken 28 hours before the 2mW point above.<sup>\*</sup>The mixing chamber temperature is obtained from an ac CMN thermometer package in conjunction with a Model KFP SQUID probe and RLM Measuring System.

ORIGINAL PAGE 1  
OF POOR QUALITY

S.H.E. CORPORATION  
DRI-420 WITH GHS-3F

nominally 440 ohms for temperatures below 4.2K; so 2 mW corresponds to 2.13 mA. The still heater used for the test is the one currently installed on the still. The still power determines the  $^3\text{He}$  circulation rate which in turn determines the refrigeration capability. However this cooling power is offset by many varied factors such as viscous heating and heat conducted down electrical leads and helium filled tubes (the still is hotter at higher still powers). Thus there is a minimum temperature, with both lower and higher still powers giving higher mixing chamber temperatures. For these data, the flow rate is measured by temporarily stopping circulation and measuring how much time is required for a 10 torr pressure rise in the known room temperature volume; see Section 4-6. The  $^3\text{He}$  to  $^4\text{He}$  ratio of the circulating helium is measured using a mass spectrometer leak detector modified to detect both  $^3\text{He}$  and  $^4\text{He}$ .

The last point in Table D-1 illustrates the existence of a heat leak into the mixing chamber which gradually decreases with time. In a period of 28 hours the mixing chamber body cooled from 7.17 mK to 6.50 mK as an equilibrium temperature for a still power of 2 mW. It is felt that this slowly decreasing heat leak might be caused by residual exchange gas, which is slowly adsorbed. For the performance test, the mixing chamber was below 4 K for only two days; further improvement might be expected for longer periods cold.

Table D-2 shows the measured refrigeration capability at a still power of 16 mW. The heat load was applied to the four wire heater currently mounted on the mixing chamber. The four wire hook-up of this heater, see Appendix A, allows both the current through the heater and the voltage drop across the heater to be measured; thus yielding an accurate determination of the heat load. The 16 mW stillpower was chosen since it produces approximately the highest circulation rate which the SHE pumping system can handle. The SHE pumping system used consists of an Edwards 9B3 booster pump backed by an Edwards ED660 sealed mechanical pump. For the lowest temperature power point, the stillpower was decreased since the resulting lower circulation rate gave a colder mixing chamber temperature for the applied heat load. The cooling power as a function of the external mixing chamber temperature is shown on the attached graph. From the smooth curve, the refrigeration capability is about 2400 erg/sec (240  $\mu$  W) at 100 mK, and 115 erg/sec at 25 mK.

The data contained in Tables in D-1 and D-2 may be very useful when first operating the refrigerator, to determine if it is running satisfactorily. It is advised not to attempt any experiments the first time the refrigerator is operated. Just operate the refrigerator to be certain its operation is understood and is satisfactory. Diagnosis of any difficulties may be much more difficult if added experimental fixtures are also present. temperature as a function of the applied heat load. From the smooth curve, the refrigeration capability is over 2700 erg/sec (270  $\mu$  W) at 100 mK, and is still about

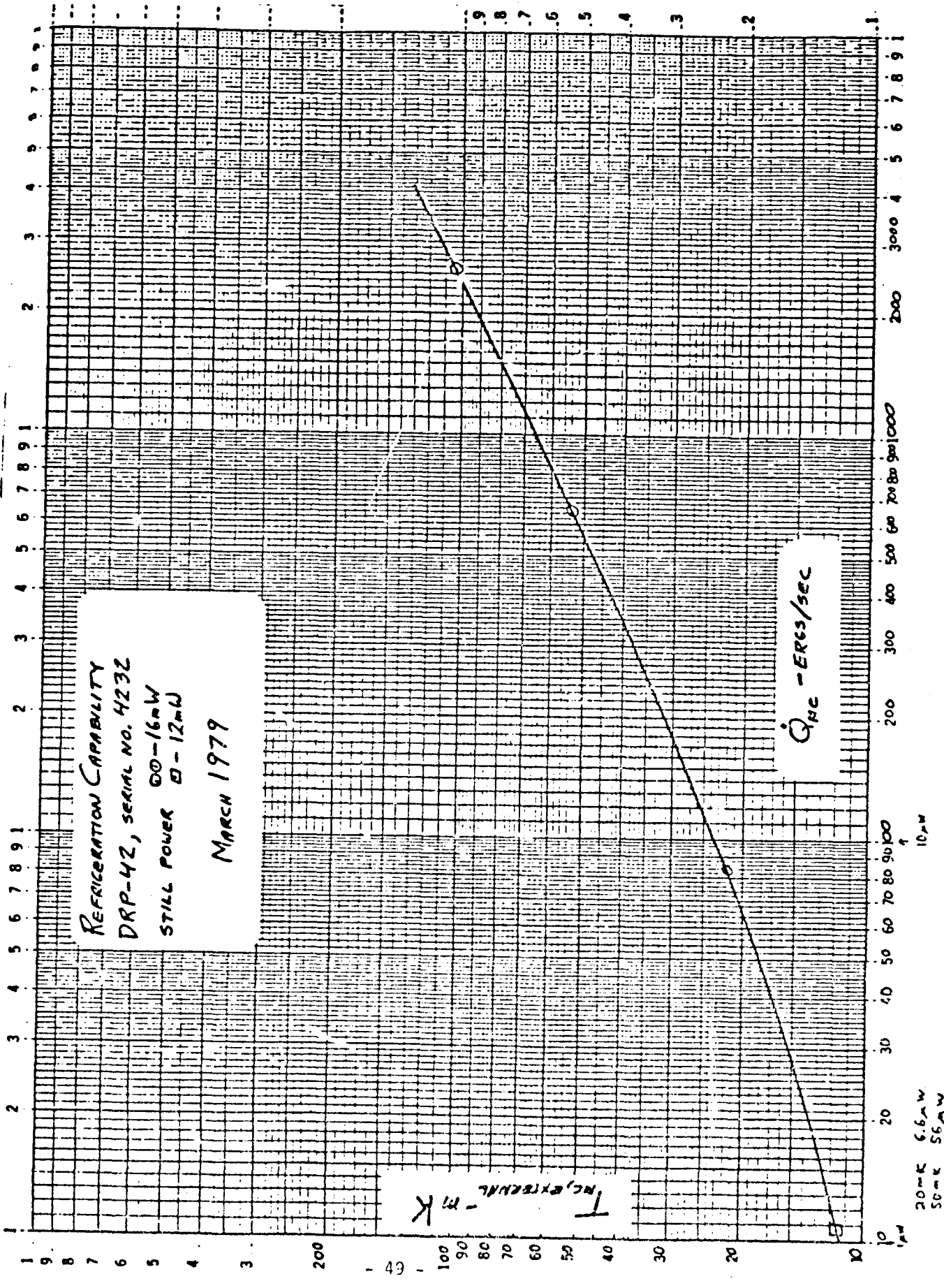
TABLE D2

Refrigeration Capability at  $\dot{Q}_{\text{still}} = 16\text{mW}$ Dilution Refrigerator Model DRP-42, Serial No. 4232

$\dot{Q}_{\text{mc}}$ erg sec	$\dot{n}$ $10^{-5}$ mole sec	Ratio $\frac{3\text{He}}{4\text{He}}$	$\dot{n}_3$ $10^{-5}$ mole sec	Condensing Pressure torr	Temperatures				
					Cold Plate K	Still K	Base Plate mK	Coldest Heat Exchanger mK	Mixing Chamber <sup>2</sup> mK INT EXT
2569	52.0	7.6	45.9	212	1.31	0.86	118	110	99.2 102.4
645	46.8	6.4	40.7	196	1.30	0.87	81	54	51.2 53.4
81.3	46.8	5.2	39.2	192	1.30	0.87	66	33	20.6 21.7
10.7 <sup>4</sup>	39.0	8.4	34.8	154	1.30	0.82	59	29	10.6 11.5

<sup>4</sup>The still power for this point was decreased to 12mW; this gave better refrigeration.

The mixing chamber temperature is obtained from an ac CMN thermometer package in conjunction with a Model MFP SQUID probe and RLM Measuring System.



S.H.E. CORPORATION  
DRI-420 WITH GHS-3F

100 erg/sec at 20 mK. For all this data, the coldplate valve was closed. However when higher still powers are used, it may be necessary to open the valve to keep the coldplate temperature acceptable.

The data contained in Tables D1 and D2 may be very useful when first operating the refrigerator; to determine if it is running satisfactorily. It is advised not to attempt any experiments the first time the refrigerator is operated. Just operate the refrigerator to be certain that its operation is understood and is satisfactory. Diagnosis of any problems may be much more difficult if added experimental fixtures are also present.

## Appendix II

Design of The milli-Kelvin cryostat and  
completion of The S.H.E. gas handling system.

## DESIGN OF MILLI-KELVIN CRYOSTAT

### STRUCTURE

A drawing of the cryostat appears in figure 16. The dimensions shown allow a final .02 K volume of  $\sim 35$  l.

The outer wall of the cryostat is at room temperature and is 25" diameter X 72" long. Inside this is the liquid nitrogen shield which is a shell formed by two co-axial cylinders of 22" and 19" diameters X 68" long. This liquid nitrogen tank has a volume of 108 l. Across the bottom of this tank is a 1/16" thick copper plate for thermal shielding. Also for thermal shielding is a 1/16" thick copper liner welded to the inside of the tank and extending 48" from the top. The entire liquid nitrogen tank is suspended from three stainless steel pipes 1/4" I.D. X 3/32" wall thickness.

Thermal considerations lead to the use of a fiberglass vessel for the inner container where the liquid helium would be. It is 16" I.D. X 70" long X 1/4" wall thickness. The vessel mates at room temperature with the rest of the cryostat with a teflon gasket. The fiberglass is made from Hetron 31, a polyester resin made by Ashland Chemicals. Typical properties of a Hetron 31 laminate are shown in table 1.

To the bottom of the liquid nitrogen tank was thermally attached a container holding  $\sim 3$  lbs of Type 5A Linde molecular sieve material. This was to absorb any residual nitrogen left in the vacuum space after pumping. A graph of the absorbance of Type 5A is shown in figure 17. Figure 18 shows the modified dilution refrigerator insert. The available experimental space inside the .3K thermal shield is an upright cylinder 16" tall X 13" diameter. This represents a volume of 35 l.

## THERMAL CALCULATIONS

### Heat Leak into the Liquid Helium

Conduction paths into the liquid helium are through the walls of the fiberglass vessel and through the support structure of the experimental insert. The thermal conductivity of the fiberglass was known only at room temperature ( $2.175 \times 10^{-3} \frac{\text{W}}{\text{cm K}}$ ). However, since the glass fibers contribute much to the properties of fiberglass, it was decided to use the thermal conductivity curve for fused quartz normalized at room temperature to the value for fiberglass. Using the data, from the American Institute of Physics Handbook, the following results were obtained for fiberglass:

$$K_{F1} \equiv \int_{4.2}^{77} \lambda(T) dT \approx .0731 \frac{\text{W}}{\text{cm}}$$

and

$$K_{F2} \equiv \int_{77}^{300} \lambda(T) dT \approx .341 \frac{\text{W}}{\text{cm}}$$

If the thermal gradient is from room temperature at the top of the cryostat to 4.2 K at the top of the liquid helium and we assume the level of helium is 24" from the top (this is the highest level), we get the heat leak from this source to be  $\dot{Q}_{c1} = .56\text{w}$ .

It is instructive at this point to compare the fiberglass vessel with a similar vessel made of stainless steel. If stainless steel were used for



the innermost shell, the minimum thickness would be 0.04". This leads to a heat leak of:

$$\dot{Q}_{S.S.} = \frac{A}{4.2} \int_{300}^{\lambda(T)} \lambda(T) dt = (.21 \text{ cm}) (30.4 \frac{W}{cm}) = 6.5W$$

Clearly, even though the fiberglass needs to be much thicker to withstand the pressure, it is still much better thermally than stainless steel.

To reduce the above heat leak even further, the fiberglass was heat sunk to the liquid nitrogen 6" from the top of the fiberglass vessel. Copper braid was wrapped around the circumference of the vessel and covered with Hetron 31 resin. This band was then connected to the liquid nitrogen tank via six copper braids equidistant around the circumference. Each copper braid was ~12" long X .48 cm<sup>2</sup> cross-section. The thermal conductivity of copper at 77 K is approximately 6  $\frac{W}{cm K}$ . If we assume that the temperature T where the braid attaches to the fiberglass is near 77 K, we can equate the power through the braid to the power through the fiberglass to find T.

$$(6 \frac{W}{cm K}) (T - 77) (.095 \text{ cm}) = (.341 \frac{W}{cm}) (5.32 \text{ cm}) (\frac{300 - T}{300 - 77}) \rightarrow T \approx 80 \text{ K}$$

where the left side of the equation is the conductivity through the copper and the right side that through the fiberglass. With the fiberglass vessel heat sunk at 80 K we find the new  $\dot{Q}_{c1} = .14 \text{ W}$ . The support for the experimental insert vacuum chamber is mainly the stainless steel pipes used for gas circulation as part of the dilution refrigerator operation. Since the dilution refrigerator was designed for a much smaller vacuum chamber than the one we will use, four 1/4" G-10 fiberglass rods were added to take up

some of the weight. The heat leak for these is:

$$\dot{Q}_{c2} = (.419 \frac{W}{cm}) (.021 \text{ cm}) = .009w$$

The total heat leak due to conductivity is  $\dot{Q}_c = .15w$ . (The heat leak due to the pipes will be considered later.)

Around the sides and bottom of the vessel were wrapped 10 layers of aluminized mylar to reduce thermal radiation. The heat leak from this is  $\dot{Q}_{R1} = 8.9 \text{ mw}$ . The inside of the vessel was plugged with styrofoam insulation to reduce convection and to channel the boil-off gas to the walls of the container. This plug consisted of 9 layers of styrofoam each ~2.5" thick sandwiched with aluminized mylar. The heat leak due to radiation from this direction would be  $\dot{Q}_{R2} = .12 w$ . The total heat leak into the liquid helium is  $\dot{Q}_T = .28 w$ .

If we assume the boil-off gas leaves the cryostat with a temperature of ~20 K the heat capacity of the helium would be ~12 KJ/liquid liter. This leads to a boil-off rate of ~2 l/day. Data from the S.H.E. Corporation indicates that the contribution to boil-off rate from the stainless steel pipes of the insert and from consumption of liquid helium in a helium cold-plate would be about 5 l/day. The total boil-off rate is, therefore, 7 l/day. Since the liquid helium volume is about 50 l, this rate should allow a 7 day running time for the dilution refrigerator.

### Heat Leak into the Liquid Nitrogen

The heat leak into the liquid nitrogen due to conduction would be through two paths. The first conduction path is the supporting stainless steel pipes. The area of these pipes is  $.653\text{cm}^2$  each. The thermal con-

ductivity for stainless steel is,  $\int_{77}^{300} \lambda(T) dT = 27.2 \frac{\text{W}}{\text{cm}}$ . If we let the

thermal gradient go from 300 K to 77 K over a distance of 1", we get

$\dot{Q}_{c1} = 21.0 \text{ w}$ . The other conduction path is the copper braid. The total area for these braids is  $2.9 \text{ cm}^2$ . If we let  $K \text{ cm} = 6 \frac{\text{W}}{\text{cm K}}$  and  $\Delta T = 3 \text{ K}$ , we get

$\dot{Q}_{c2} = 1.7 \text{ w}$ . The total heat leak due to conduction into the nitrogen is

$\dot{Q}_c = 22.7 \text{ w}$ .

The liquid nitrogen tank is also insulated with 10 layers of aluminized mylar. The radiation heat leak from room temperature is  $Q_R = 2.9 \text{ w}$ . The total heat leak into the liquid nitrogen is, therefore,

$$\dot{Q}_T = 25.6 \text{ w}.$$

If we assume the boil-off gas leaves the cryostat at 100 K, we get a boil-off rate of 11 l/day. Since the copper thermal shield extends only to 48" from the top, we will assume the tank is empty when the level reaches that point. This represents a volume of 76 l and also gives a running time of about 7 days.

These calculations indicate that, with this cryostat, an experiment may be run for about a week without the noisy interruption of adding cryoliquids.

#### COMPLETION OF THE GAS HANDLING SYSTEM

The dilution refrigerator purchased from the S.H.E. Corporation includes a Gas Handling System (GHS) which controls the flow of  $\text{He}^3$  and  $\text{He}^4$  into the dilution refrigerator. An option offered by SHE is to buy only that part of the GHS which handles the more expensive  $\text{He}^3$ . In order to obtain a more powerful refrigerator we purchased the half system. The second half of the GHS is used for pumping and purging with  $\text{He}^4$  and  $\text{N}_2$ . We have just completed construction of this portion so as to have all the capabilities of the complete GHS. This completed GHS gives us one of the most powerful dilution refrigerators commercially available and should allow us to reach temperatures  $< 20\text{mK}$ .

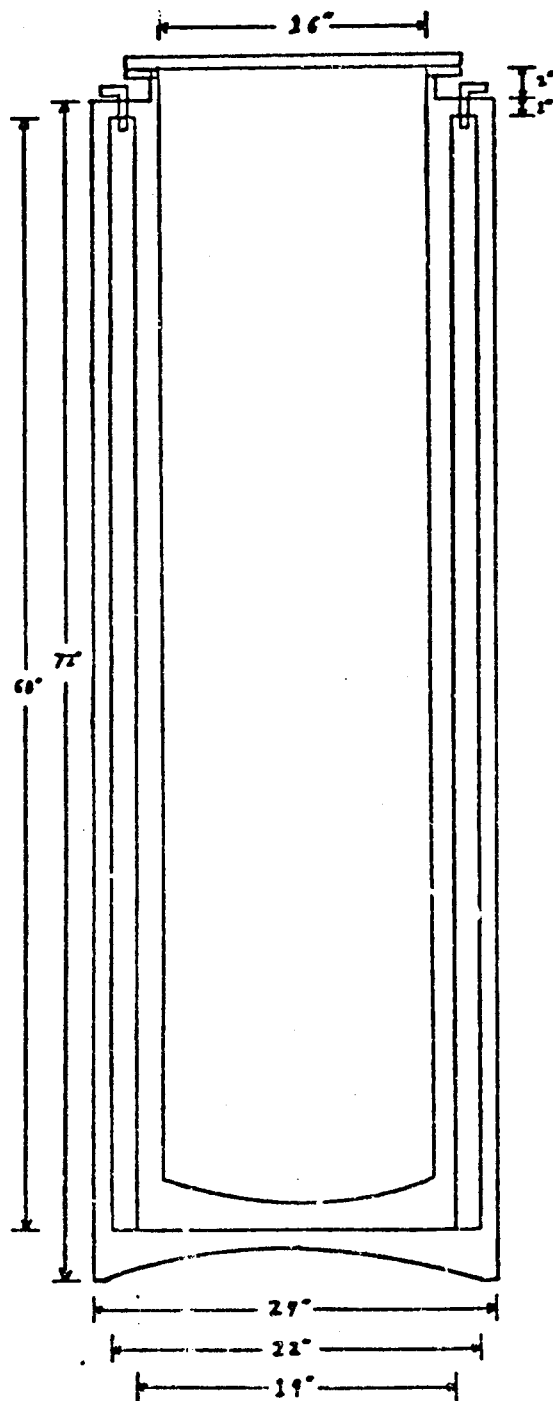


Figure 16. Milli-Kelvin cryostat

ISOTHERM DATA SHEET NO. 62  
 ADSORBATE: Nitrogen  
 TEMPERATURE:  $-196^{\circ}\text{C}$  to  $-75^{\circ}\text{C}$

TITLE: Nitrogen Adsorption  
 ADSORBENT: Molecular Sieve Type 5A Pellets

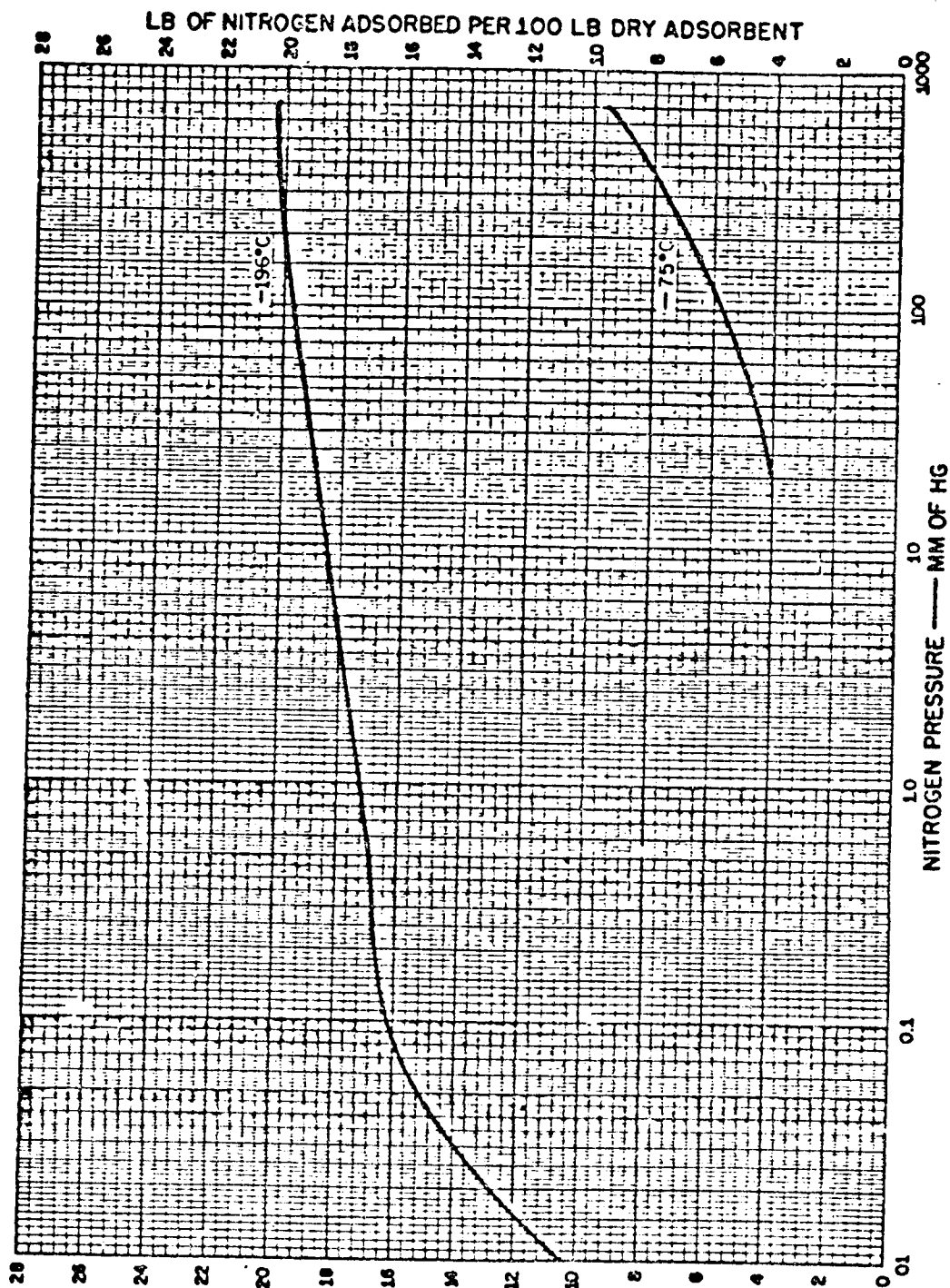


Figure 17. Linde type 5A molecular sieve adsorbance



ADSORBENTS  
 & CATALYSTS

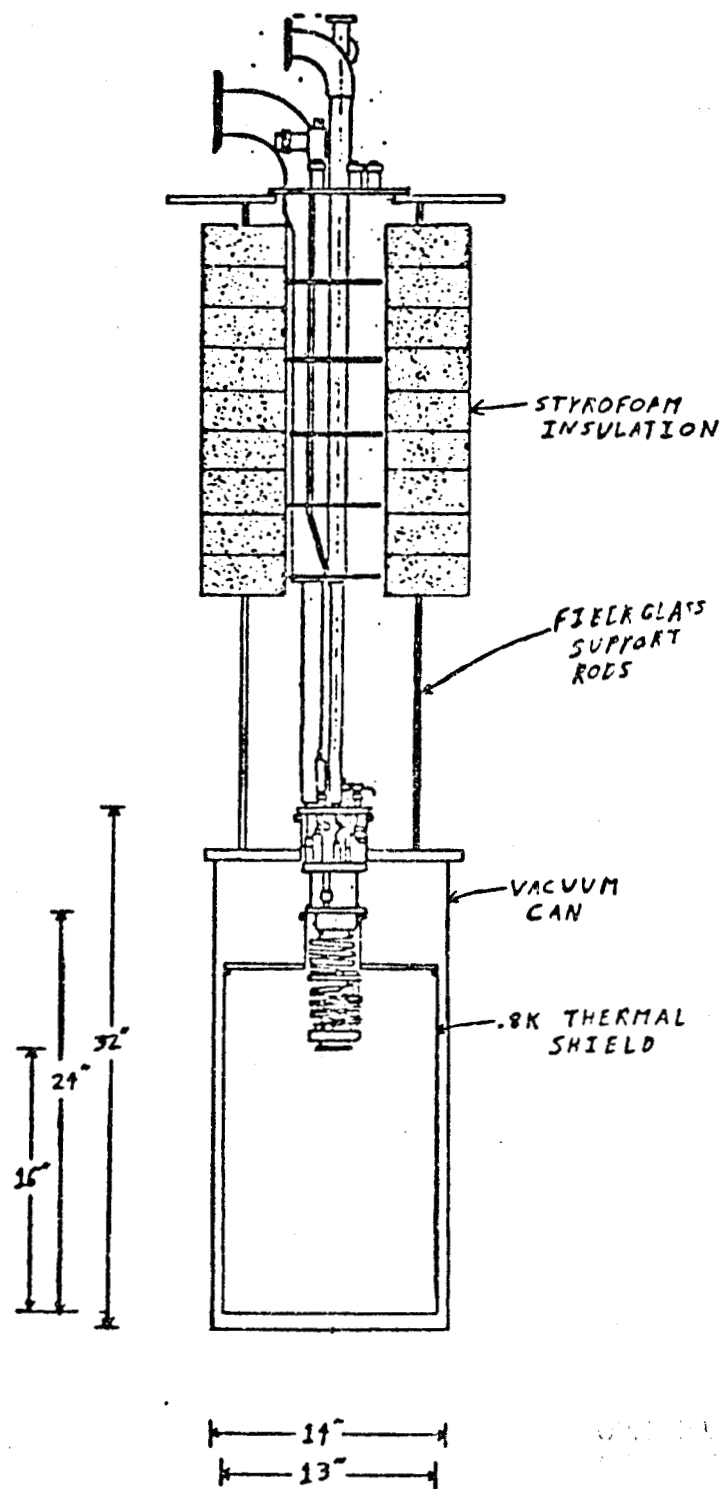


Figure 18. Dilution refrigerator insert and vacuum can

# HETRON 31 LAMINATES

60% Glass Cloth, 181 Volan A, Press Cured, 1/8 inch

## TENSILE PROPERTIES (Average of 5)

	<u>R.T.</u>	<u>-110°F</u>	<u>-320°F</u>	<u>-424°F</u>
Ultimate Strength x 10 <sup>3</sup> psi	50.0	68.1	105.3	100.0
Initial Modulus x 10 <sup>6</sup> psi	2.97	3.24	3.87	3.92

## FLEXURAL PROPERTIES (Average of 5)

Ultimate Strength x 10 <sup>3</sup> psi	71.2	104.1	126.7	129.0
Initial Modulus x 10 <sup>6</sup> psi	3.24	3.47	4.18	4.26

## EDGEWISE COMPRESSION PROPERTIES (Average of 5)

Ultimate Strength x 10 <sup>3</sup> psi	19.9	41.2	68.5	67.3
Modulus x 10 <sup>6</sup> psi	1.64	1.85	2.36	2.71

Table 1. Hetron 31 fiberglass properties